Answers Research Journal 7 (2014):49–81.
www.answersingenesis.org/arj/v7/radiohalos-bathurst-batholith-granite-flood.pdf

ARJ

Radiohalos in Multiple, Sequentially Intruded Phases of the Bathurst Batholith, NSW, Australia: Evidence for Rapid Granite Formation during the Flood

Andrew A. Snelling, Answers in Genesis, P.O. Box 510, Hebron, Kentucky, 41048.

Abstract

The Bathurst Batholith west of Sydney, Australia, consists of an enormous pluton (the Bathurst Granite) and numerous smaller related satellite plutons and dikes. The major pluton cuts east-west across the prevailing north-south strike of the fossiliferous sedimentary strata, unequivocal evidence that the intrusion of the batholith structurally disrupted the regional fabric of the host strata sequence. Sedimentary rocks in the contact zone were metamorphosed by the hot magma. The major dike-like Evans Crown granite cuts across the Bathurst Granite and the surrounding host strata. This dike's central portions are coarse and even grained like the Bathurst Granite, but the margins are chilled, testimony to intrusion of the dike as hot granite magma. Many minor granite dikes cut across the margins of the Bathurst Granite and also across the Evans Crown dike out into the surrounding strata. Alteration zones marginal to the sharp contacts of the dikes with the wallrocks indicate the magma was still hot when injected. Abundant ^{238}U and ^{210}Po radiohalos are present in biotite flakes of all samples of the Bathurst Granite and Evans Crown dike. ^{214}Po and ^{218}Po radiohalos are present only in some samples of the Bathurst Granite. A few ^{210}Po and ^{238}U radiohalos are also present in biotite flakes within some samples of the dikes that cut across the Bathurst Granite or the Evans Crown dike. Field and textural data have established that these granite phases were sequentially intruded while still hot. That these granitic phases were intruded as hot magma is also confirmed by analytical and experimental data. All this had to occur within the Flood year, so these multiple granite phases were not created cold by fiat. Instead, the Po radiohalos indicate they were formed rapidly below 150°C via hydrothermal fluid transport of Rn and Po from the zircon grains embedded in the biotite flakes that are often the radiocenters of the U radiohalos. Furthermore, their presence in all three sequentially intruded granite phases is evidence that all this intrusive activity, and the cooling of all three granite phases to 150°C, must have occurred within a week or two so that these Po radiohalos in them formed subsequently within days to weeks.

Keywords: granite, Bathurst Batholith, magma, contact metamorphism, dikes, alteration zones, host fossiliferous sediments, chemical analyses, experimental data, biotite, ^{238}U radiohalos, Po radiohalos, hydrothermal fluids, the Flood

Introduction

Over 50 years ago there was intense debate in the conventional scientific community on the origin and formation of granites (Pitcher 1993). For most geologists it has now been conclusively resolved that granitic magmas formed by partial melting of deep crustal (continental) rocks or of subducted sediments at temperatures of around 630–730°C. The hot granitic magmas, being less dense than the surrounding source rocks, then ascended through fractures and feeder zones to intrude into upper crustal rocks, including fossiliferous sedimentary strata. Often, the heat and hydrothermal fluids released by the cooling granitic magmas baked and/or altered the host rocks around the contact zones (contact metamorphism and/or metasomatism).

However, there are still some unresolved issues. On one hand, there is the issue of the time involved for such a process, because the conventional geologic community generally regards the time necessary from partial melting to intrusion, crystallization and cooling of granites to have taken millions of years (Pitcher 1993; Young and Stearley 2008). On the other hand, a potential solution to the time issue and an alternative model for the origin of granites was presented by Gentry (1973, 1974, 1986, 1988). He argued that because the polonium (Po) radiohalos within biotite grains in granites appeared to be "orphaned" (there apparently being no precursor or parent atoms in situ), and they thus had to form extremely rapidly (due to the fleeting existence of two of the polonium isotopes), the Po radiohalos and the granites hosting them had to have been created in a fiat manner by God. He concluded the granites are primordial rocks and termed the Po radiohalos as God's "fingerprints of creation."

The observation that many granite bodies intrude fossil-bearing sedimentary rocks which were deposited during the Flood is not considered an obstacle to this proposal for the instantaneous origin of granites. Instead, Gentry (1986, 1988, 1989) proposed and insisted that primordial granite bodies were tectonically intruded during the Flood while they were cold, and any thermal effects surrounding

the margins of these granite bodies was due to frictional heating during tectonic emplacement. His argument was aided by the observational fact that limited exposures of the contact zones at the margins of granite bodies are difficult to find. However, this is because outcrops of the contact zones are often not fully exposed or are absent due to the alteration effects facilitating deeper weathering of both the margins of the granite bodies and their adjacent host rocks.

A number of previous studies have sought to establish the case for Po radiohalos having formed rapidly from Po atoms sourced from nearby decaying uranium (U) atoms and transported by hydrothermal fluids during the cooling phase of granite bodies (Snelling 2005a, 2008a, d; Snelling and Armitage 2003; Snelling and Gates 2009). Only one of these studies included an investigation of the contact zone around a granite body. Also, no previous studies examined discrete, separate granite bodies that had intruded into one another sequentially. The present study encompasses these two aspects in the investigation of a major granite body, two generations of dikes intruding into it, and their contained radiohalos.

Fieldwork was conducted in July–September 1974 as the focus of a B.Sc. (Honors) dissertation at The University of New South Wales, Sydney, Australia, in an area located about 185 km (115 mi.) west of the city of Sydney (fig. 1). Detailed field observations were made of the contact zone along the margins of the Bathurst Granite where it intruded the host fossil-bearing sedimentary strata, and where it was itself intruded by two generations of late-stage granitic dikes. The resulting unpublished dissertation (Snelling 1974) was a description and discussion of the geology of the field area, accompanied by the compiled geological map. Further fieldwork in the region was undertaken in July 1999 to acquire a regional perspective in the investigation of radiohalos in the granite and the dikes. This subsequent radiohalos study used samples collected in 1999 and archived samples from the 1974 dissertation fieldwork. The results provide convincing evidence that this granite and its ancillary phases were indeed intruded rapidly as a hot magma into the surrounding host fossiliferous sedimentary strata during the Flood. Furthermore, the radiohalos in these sequentially intruded phases had to have been produced rapidly from Po atoms sourced from decaying U atoms in these granitic rocks.

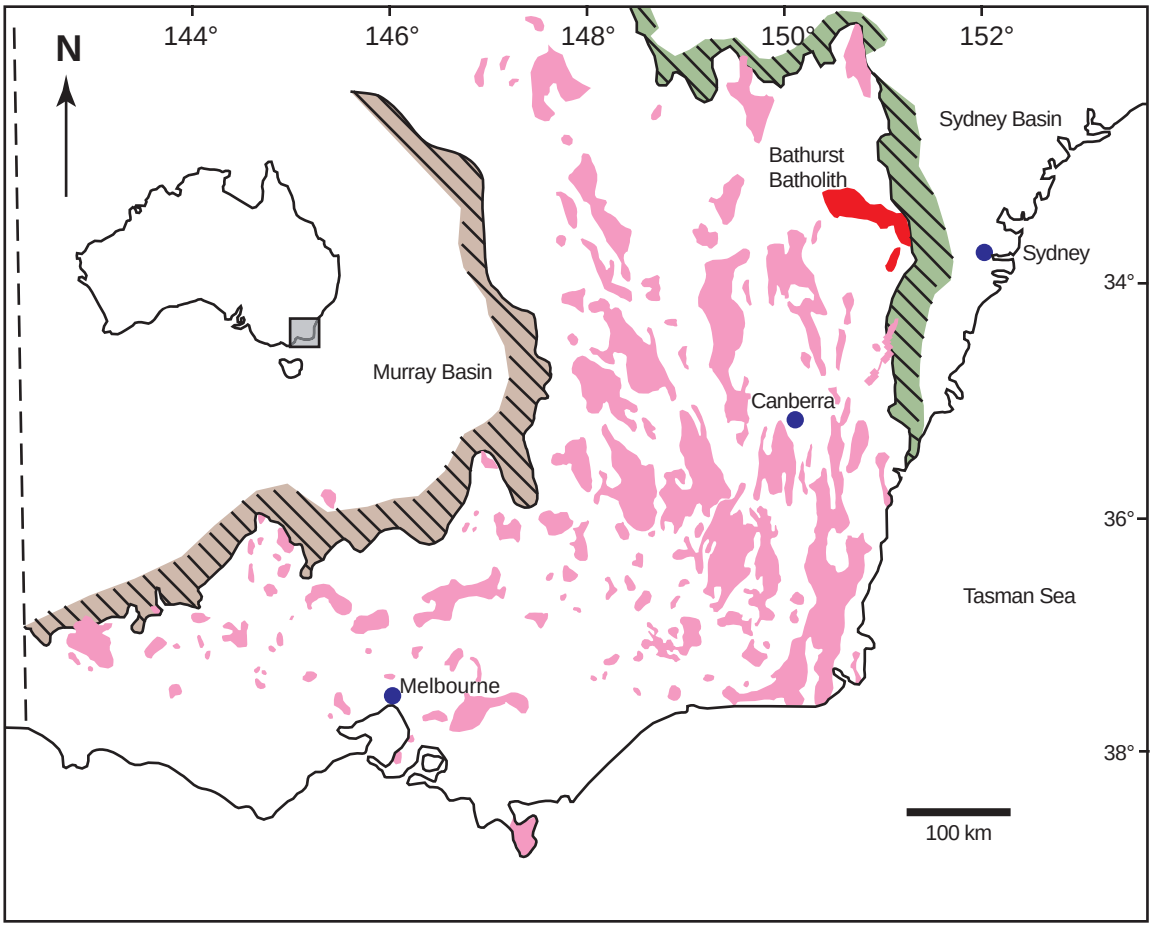

Fig. 1. Location of the Bathurst Batholith (red) in relation to other granite batholiths (pink) in south-eastern Australia.

The Bathurst Batholith

Geologic setting

The Bathurst Batholith, named after the city which sits on top of it, outcrops over an area of about 1600 km^2 (620 sq. mi.) (fig. 1). It consists of an enormous pluton (the Bathurst Granite) and numerous smaller related satellite plutons and dikes. Though often deeply weathered, the granite is well exposed in road and railroad cuts, and in the hills around its margins which have been mapped in detail. At the contact with the granite the host fossiliferous sedimentary strata have been metamorphosed and in this instance have thus been more resistant to weathering (Joplin 1936; Snelling 1974; Vallance 1969).

Previous studies by Chaffer (1955) and Mackay (1959) included geological mapping and investigations, as well as the measuring of the type section for the Lambie Group at Mt. Lambie in the map area and identifying the fossil assemblages.

Outcrops are poor over much of the Bathurst Plains and little is known of the granite in that region. However, early fieldwork by Joplin (1931, 1933, 1935, 1944) dealing with the eastern part of the batholith has contributed much to our knowledge of the batholith as a whole as a composite body, concluding the batholith consists of multiple plutons with variable compositions ranging from minor gabbroic phases to dominant adamellite (Chappell et al. 1991; Joplin 1931; Knutson and Flood 1988; Vallance 1969). The main plutonic rock types in the eastern part of the batholith, as elsewhere in the batholith, are pinkish, even-grained, biotite-granite/adamellite, gray biotite-granite/adamellite with large pink phenocrysts of potassium feldspar, hornblende-biotite granite/adamellite, and hornblende and biotite granodiorites (Joplin 1931). All are medium- to coarse-grained and massive with gradational contacts between the several varieties. Biotite granites with large potassium feldspar phenocrysts outcrop, for example, near Sodwalls and Tarana in the area studied by Snelling (1974). The satellite stock-like body at Yetholme, which appears to be related to the main mass of the batholith, also carries similar large K-feldspar phenocrysts.

In general, age relations between the various granitic units in the batholith are not clear. An obvious exception to this rule is the major dike-like granite body 12.8 km (8 mi.) long and often 0.8 km (0.5 mi.) wide that forms the Evans Crown ridge near Tarana and extends north-north-eastwards cutting across the Bathurst Granite and the surrounding host sedimentary strata. Numerous minor granitic dikes cut across the margins of the Bathurst Granite and out into the surrounding host strata. Good exposures of these dikes are seen in the many railroad cuts between Sodwalls and Tarana. Up to 45 m (about 150 ft.) wide, these granitic dikes have the same composition as both the Bathurst Granite and the Evans Crown dike, often with the same porphyritic texture (Snelling 1974).

Recent airborne magnetic and radiometric surveys have enabled the separate bodies with different compositions to be identified within the main outcrop of the batholith (Branagan and Packham 2000). The individual intrusive phases are well expressed on modern detailed aeromagnetic maps and in radiometric data. Detailed mapping using such data combined with petrology has enabled their improved depiction on geological maps (Raymond et al. 1998). The emplacement of these granitic plutons caused thermal metamorphism (hornfels and skarns) and metasomatism to the surrounding strata.

Earlier K-Ar dating (Facer 1979) on an adamellite from Dunkeld just east of the city of Bathurst, yielded a total rock age of 304±4Ma and a biotite age of 301±6Ma for the western part of the Bathurst Granite, has proved unreliable. Radioisotope dating using the K-Ar, Rb-Sr, and Re-Os methods has been interpreted as indicating a mean time of emplacement of the Bathurst Batholith at 310Ma (Scheibner and Basden 1998). However, Shaw and Flood (1993) have suggested that these ages are too young. Shaw's unpublished data (Scheibner and Basden 1998) consists of more extensive Rb-Sr age dating of biotite/bulk rock pairs, and show that all plutons are older, with the mafic intrusions being the oldest at 340Ma (Knutson and Flood 1988). This is within the range of 338–349Ma from biotite in the regionally metamorphosed Merrions Formation (Cas, Flood, and Shaw 1976). The youngest intrusives dated are the felsic north-south dikes cross-cutting the Bathurst Batholith, with the Evans Crown dike dating at 312Ma. Shaw and Flood's (1993) histogram of 33 biotite ages from all major plutons of the batholith suggests an intrusive maximum around 325–330Ma.

In its structural setting the Bathurst Batholith is clearly discordant along much of its margin. Apart from radiometric dating, the evidence that the granite intruded later than the folding can be seen in the shape of the granite body which trends east-west, cutting across the "grain" of the folded host sedimentary rocks (fig. 2). The western part of the batholith lies against well-cleaved or foliated lower Paleozoic rocks. In places, the host country rocks have been shoved locally into concordances with the trend of the contact. Important structural features such as the thrust fault systems to the north of the batholith are intersected by the intrusive body which is clearly younger than the thrust faults.

The granitic bodies making up the batholith invade host country rocks as young as upper Devonian, and on the eastern margin are overlapped by Permian sediments. The available evidence from the thickness

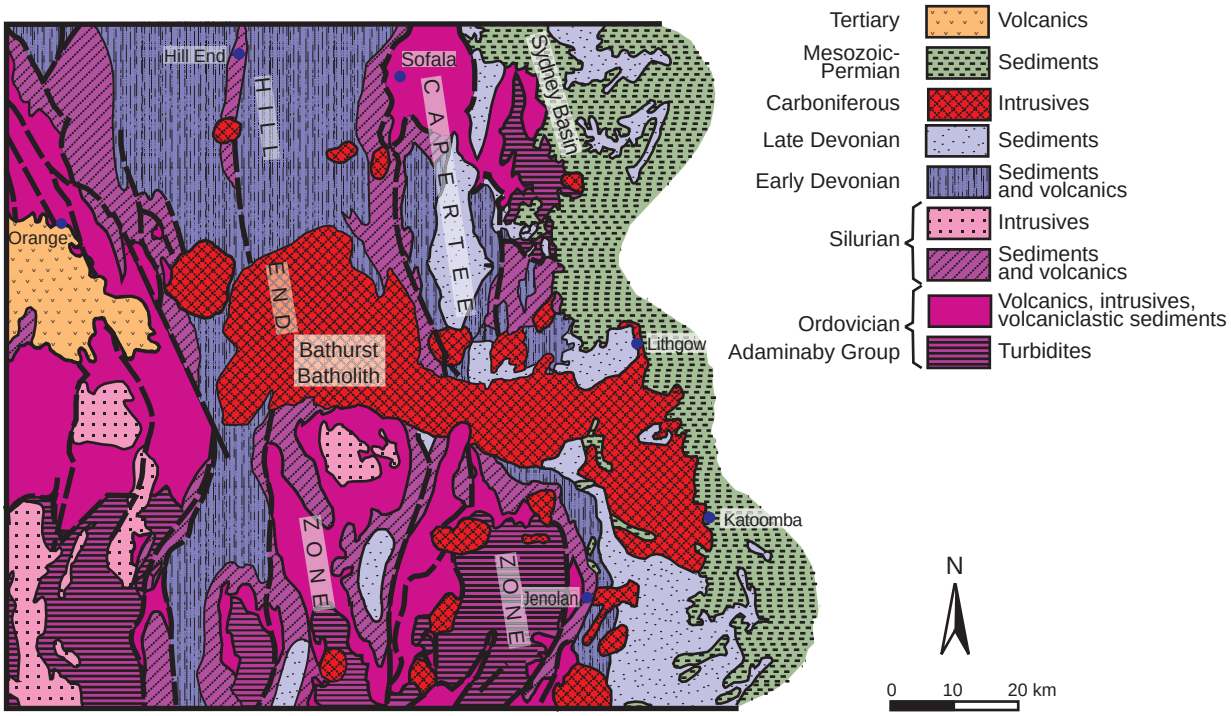

Fig. 2. Simplified geological map of the Lachlan Fold Belt in the region of the Bathurst Batholith (after Branagan and Packham 2000).

of the overlapping Permian sediments suggests that the depth of cover at the eastern margin, at least, was not great, perhaps not more than 1.5 km (0.93 mi). The distribution of the thermal aureole indicates that the contacts between the granites and the host sedimentary strata are often rather shallowly-dipping, as can clearly be recognized in the Tarana area. The numerous stocks, including those at Yetholme and Meadow Flat, which are lithologically similar to the rocks of the main granite mass of the batholith, yet separated from it at today's land surface, suggest that the granite is not deeply eroded.

With the folding and regional metamorphism of the sedimentary strata in what is now the Lachlan Fold Belt, numerous post-kinematic, massive, orogenic granites were intruded into these host strata, including the Bathurst Granite. These granites cut across the structural zones, and individual granitic stocks and batholiths show a marked preference for zones of crustal weakness, such as pre-existing lineaments and fracture zones. For example, the transverse Bathurst Batholith was emplaced along the Lachlan River Lineament (Scheibner and Stevens 1974). Aeromagnetic data indicate the importance of some additional lineament directions for the emplacement history of the Bathurst Batholith (Raymond et al. 1998). Also, the individual plutons, their often concentric structure and the numerous late north-south trending dikes, which are also very common in the surrounding country rocks, are all well displayed in the aeromagnetic images.

Host rocks the batholith intrudes

The Bathurst Batholith and related satellite bodies and dikes intrude into folded Silurian-Devonian marine sediments and pyroclastics. Two tectonically distinct zones are recognized in the local region—the Hill End Trough and the Capertee High (fig. 2). The Hill End Trough was the site of thick active sedimentation—almost 7500 m (24,600 ft.) of turbidites, flysch, and pyroclastics (Scheibner and Basden 1998). These sediments thin and wedge out as they onlap the Capertee High, which is believed to have been the site of the active volcanism responsible for much of the pyroclastic material and lava flows in the sedimentary sequence.

At the base of the stratigraphic section in the mapped area is the Silurian Chesleigh Group (Scheibner and Basden 1998) (fig. 3) which crops out sparsely south and east of Meadow Flat (fig. 4) and in its type area is 1050 m (3445 ft.) thick (Packham 1968). It consists of turbidites, primarily graywackes (well-sorted with small angular quartz and feldspar fragments scattered throughout a clay matrix) with interbedded shales (typically composed of extremely small grains of quartz and occasional feldspar set in a clay matrix). Up-sequence the amount of feldspar increases, and these turbidites are interbedded with felsic tuffs, characterized by quartz, orthoclase and plagioclase fragments in an ultra-fine groundmass. Among the tuffs is a porphyritic rhyodacite lava, consisting of fragmented quartz, orthoclase and plagioclase phenocrysts in a flow-banded groundmass.

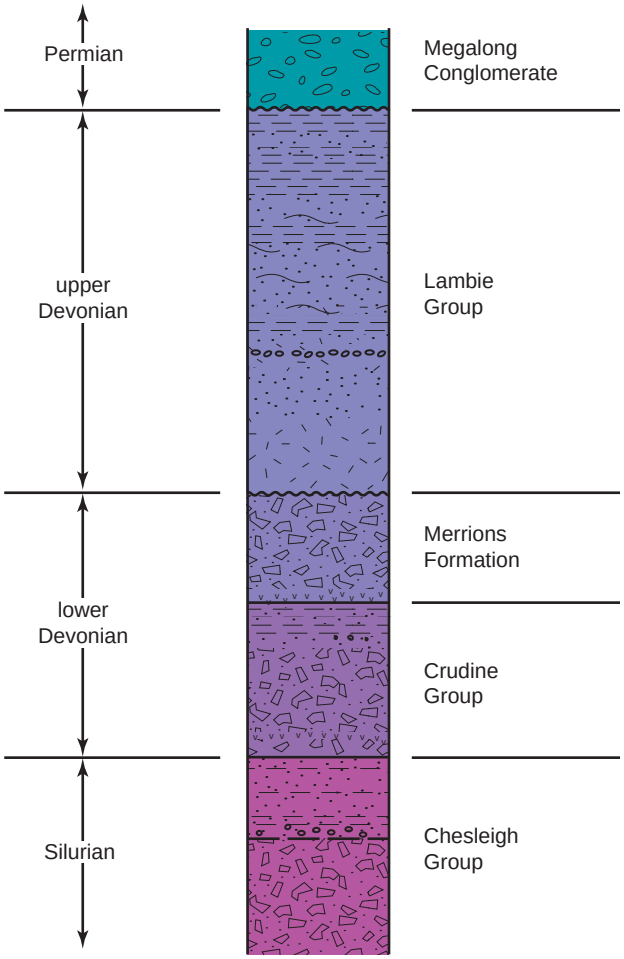

Fig. 3. The local stratigraphic column (approximately 6100 m [20,000 ft] thick), showing the order of deposition of the sedimentary rock units that host the Bathurst Granite in the Tarana-Sodwalls area.

There is a sharp change in the conformably overlying lower Devonian Crudine Group from quartz-rich sedimentation into volcanogenic deposition of felsic tuffs, tuffaceous breccias, banded tuffs interbedded with graywackes, siltstones, and shales. Then followed the accumulation of the widespread, grossly tabulated volcanogenic Merrions Formation (fig. 3), which consists of sheet-like to lobate horizons of dacite lavas and volcaniclastics. These two lower Devonian stratigraphic units are together about 1600 m (5250 ft.) thick in the study area (Snelling 1974)

In the middle Devonian the sediments deposited in the Hill End Trough and on adjoining highs were deformed regionally into north-south trending folds with an axial slaty cleavage. This was followed by onset of upper Devonian molassic sedimentation with deposition of the Lambie Group (fig. 3). In the type section on Mt. Lambie, Mackay (1959, 1961) measured 3405 m (11,170 ft.) of reddish shales, siltstones, sandstones, conglomerate and massive quartzites. Upper Devonian fossils recorded in the area include brachiopods (including four species of *Cryptospirifer*), clams and clam fragments. The Bathurst Granite is in direct intrusive contact with the upper Devonian Lambie Group strata, so the granite is clearly younger. However, unconformably overlying all these Silurian-Devonian sedimentary units and the Bathurst Granite on its eastern flank is the Permian Megalong Conglomerate, a massive cobble conglomerate which is the basal unit of the western Sydney Basin (fig. 2).

Metamorphism in the host rocks

Exogenetic metamorphic products associated with the batholith are variable. Many previously cleaved or foliated rocks have retained traces of original structures after static recrystallization. Thus in the Newbridge area, on the extreme southwestern margin of the batholith (Benson 1907), and to the north of the batholith (Vallance 1969), slates develop porphyroblasts of andalusite or chiastolite. On the southern margin of the batholith, some reaction between foliated rocks and the granite has led locally to the formation of banded quartzofeldspathic rocks described as migmatites by Binns (1958).

To the east, the batholith comes into contact with less deformed rocks, and massive granoblastic hornfelses are typical in the aureole. Similar products have been examined in detail at Hartley (Joplin 1935), where the upper Devonian sediments include quartz-rich sandstones, shales and impure calcareous rocks. Among the sandstone and shale hornfelses, the most common minerals are quartz, biotite, andalusite, and cordierite. More calcareous rocks include plagioclase, diopside, hornblende, wollastonite, grossular, or vesuvianite. Local variations in grade are common and not all hornfelses carry equilibrium assemblages. Andalusite-biotite-potassium feldspar hornfelses (indicating pyroxene hornfels facies conditions) and hornblende-diopside-plagioclase rocks (hornblende-hornfels facies) both occur at Hartley (Joplin 1935, 1936). At granite contacts near Tarana, calc-silicate rocks are derived from limestones. Silicated hornfelses (andradite-wollastonite) occur between recrystallized pure limestone and granite suggesting transfer of material across the contact. Andradite-hedenbergite skarns occur at various localities, such as at Yetholme where a satellite stock has invaded a succession containing limestones and conglomerates with limestone pebbles (Vallance 1969).

History and Significance of U and Po Radiohalos

When radiohalos were first reported between 1880 and 1890, they remained a mystery until the discovery of radioactivity. Now they are recognized as any type of discolored radiation-damaged region

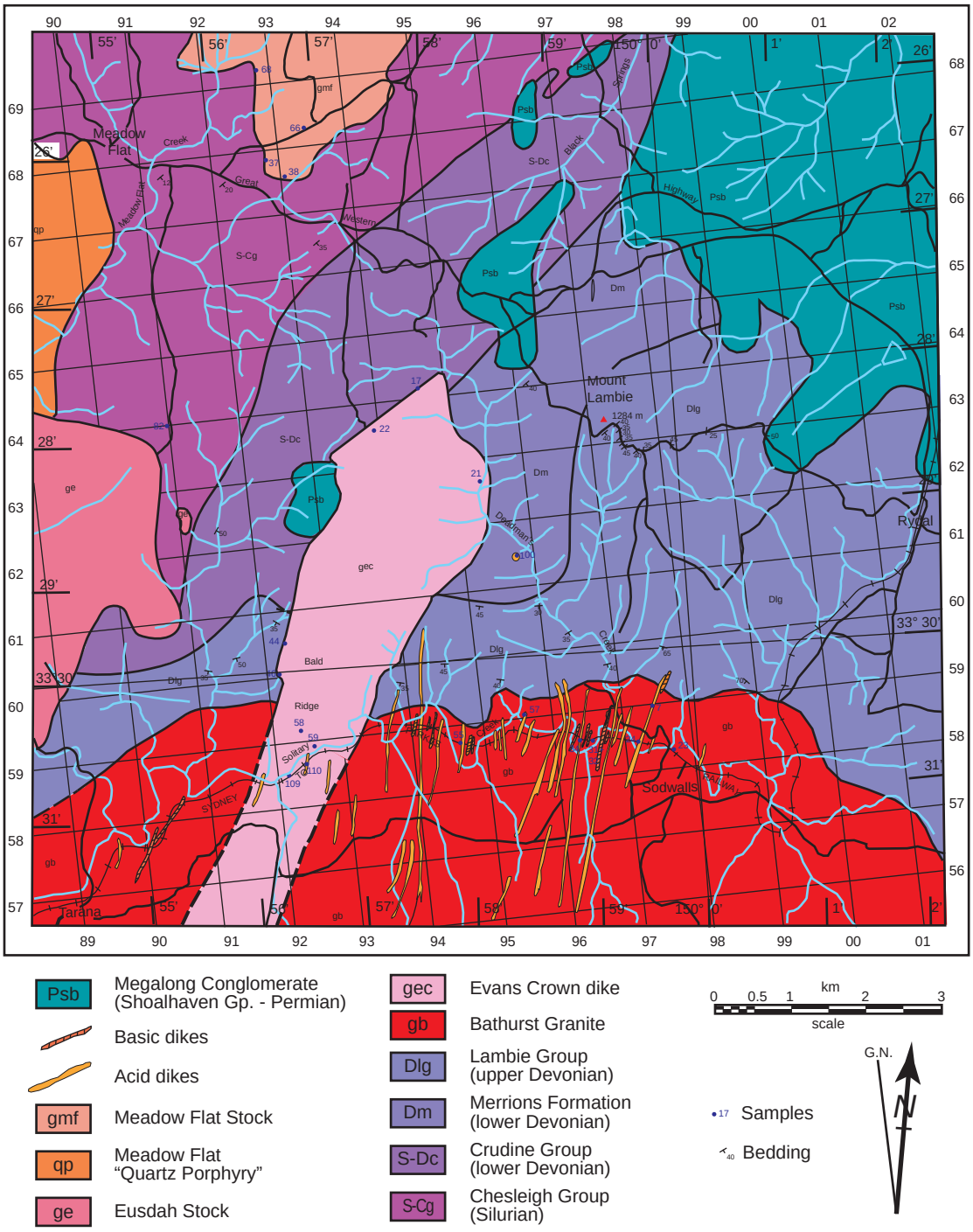

Fig. 4. Geological map of the Tarana-Sodwalls-Mt. Lambie-Meadow Flat area, west of Sydney, New South Wales, Australia (from Snelling 1974).

within a mineral, resulting from the α-emissions from a central radioactive inclusion or radiocenter (Gentry 1973). Radiohalos when viewed in rock thin sections usually appear as concentric rings that were initiated by the α-decay in the ^{238}U or ^{232}Th series (Gentry 1973, 1974). Radiohalos are usually found in igneous rocks, most commonly in granitic rocks in which biotite is a major mineral. However, more recently radiohalos have also been reported as common in biotite in some metamorphic rocks (Snelling 2005a, 2008b, c). Thus biotite is the major mineral in which the radiohalos occur. While initially observed mainly in Precambrian rocks (Gentry 1968, 1970, 1971; Henderson and Bateson 1934; Henderson, Mushkat, and Crawford 1934; Iimori and Yoshimura 1926; Joly 1917a, b, 1923, 1924; Kerr-Lawson 1927, 1928; Owen 1988; Wiman 1930), radiohalos have since been shown to exist in rocks stretching from the Precambrian to the Tertiary (Holmes 1931; Snelling 2000, 2005a; Stark 1936; Wise 1989).

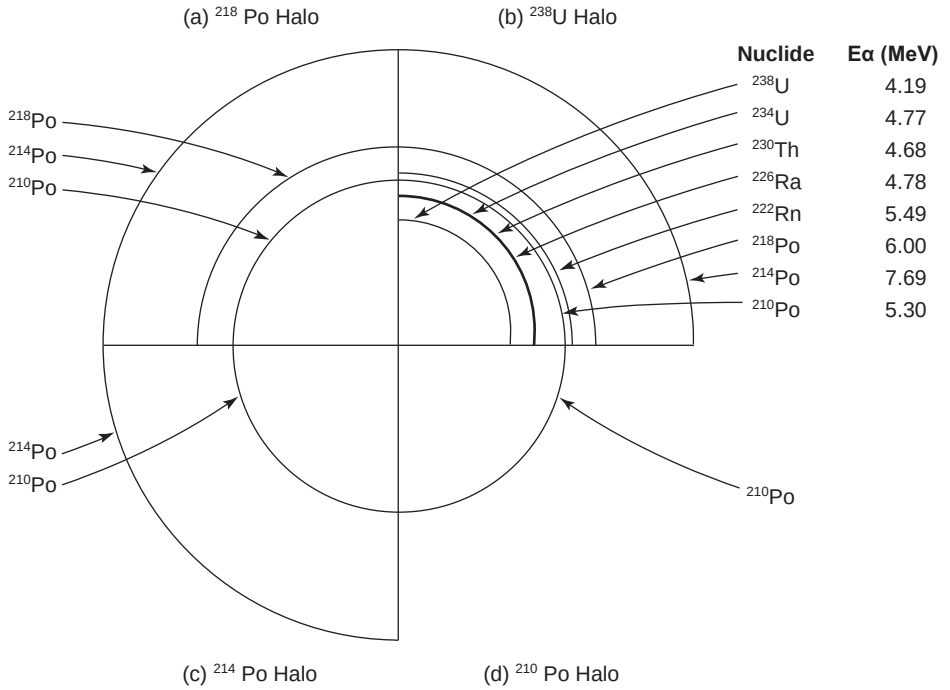

Fig. 5. Composite schematic drawing of (a) a ^{218}Po halo, (b) a ^{238}U halo, (c) a ^{214}Po halo, and (d) a ^{210}Po halo, with radii proportional to the ranges of the α-particles in air. The nuclides responsible for the α-particles are listed for the different halo rings (after Gentry 1973).

Within the ^{238}U decay series, the three Po isotopes have been the only α-emitters observed to form radiohalos other than ^{238}U itself (fig. 5). These isotopes and their respective half-lives are ^{218}Po (3.1 minutes), ^{214}Po (164 microseconds), and ^{210}Po (138 days), respectively. Their very short half-lives constrain the formation of the granites in which they are found to a short time frame because the Po radiohalos can only form after the granites have crystallized and cooled (Gentry 1986, 1988; Snelling 2000, 2005a). Thus, if granite magma emplacement and pluton cooling are not extremely rapid, then these Po isotopes would not have survived to form the Po radiohalos (Snelling 2008a). This is consistent with, and in support of, a young earth model.

Because the rings which should be produced by the Po precursors are missing in many Po radiohalos (fig. 5) (Snelling, Baumgardner, and Vardiman 2003), the source of the Po for the radiohalos has been an area of contention (Snelling 2000). Was it primary, or did a secondary process transport it? Gentry (1986) proposed that the Po radiohalos had been produced by primordial Po, having an origin independent of any U, suggesting all granites and granitic rocks were formed by fiat creation during the Creation week. In contrast, based on all the available evidence, Snelling (2000) suggested a possible model for transporting the Po via hydrothermal fluids during the latter stages of cooling of granite plutons to sites where the Po isotopes would have been precipitated and concentrated in radiocenters that then formed the respective Po radiohalos in the granites.

Subsequently, Snelling and Armitage (2003) investigated the radiohalos in biotite within three granite plutons, demonstrating that these granite plutons had been intruded and cooled during the Flood. They found that the biotite grains contained both fully formed ^{238}U and ^{232}Th radiohalos around zircon and monazite inclusions (radiocenters) respectively, thus providing a physical, integral, historical record of at least 100 million years' worth (at today's rates) of accelerated radioactive decay during the recent year-long Flood. However, Po radiohalos were also often found in the same biotite flakes as the U radiohalos, usually less than 1 mm (0.04 in) away. Thus, they argued that the source of the Po isotopes must have been the U in the zircon grains within the biotite flakes, the same zircon inclusions that are the radiocenters to the U radiohalos.

Because the precursor to ^{218}Po is the inert gas ^{222}Rn, which is produced by ^{238}U decay in the zircon grains and is then capable of diffusing out of the zircon crystal lattice, Snelling and Armitage (2003) reasoned that the evidence confirmed the tentative model suggested by Snelling (2000). Concurrently, as the emplaced granite magma crystallizes and cools, the water dissolved in it is released below 400°C, causing hydrothermal fluids to begin flowing around the constituent minerals and through the granite pluton, including along the cleavage planes within the biotite flakes. Snelling and Armitage (2003) and Snelling (2005a) argued these hydrothermal fluids were capable of transporting ^{222}Rn (and its daughter Po isotopes) from the zircon inclusions to sites

where new radiocenters were formed by Po isotopes precipitating in lattice imperfections containing rare ions of S, Se, Pb, halides or other species with a geochemical affinity for Po. Continued hydrothermal fluid transport of Po would have also replaced the Po atoms in the radiocenters as they α-decayed to produce the Po radiohalos, thus progressively supplying the 5×10^9 Po atoms needed to form fully registered Po radiohalos.

Significantly, none of the radiohalos (Po or U) could form or be preserved until the biotite crystals had formed and cooled below the thermal annealing temperature for α-tracks of 150°C (Laney and Laughlin 1981). Yet hydrothermal fluids probably started transporting Rn and the Po isotopes immediately after they were expelled from the crystallized granite at temperatures below 400°C. This implies that cooling of the Po-radiohalo-containing granite plutons had to be extremely rapid, in only 6–10 days (Snelling 2008a). Snelling, Baumgardner, and Vardiman (2003) and Snelling (2005a) have summarized this model for hydrothermal fluid transport of U-decay products (Rn, Po) in a six-step diagram. The final step concludes with the comment:

> With further passing of time and more α-decays both the ^{238}U and ^{210}Po radiohalos are fully formed, the granite cools completely and hydrothermal fluid flow ceases. Note that both radiohalos have to form concurrently below 150°C. The rate at which these processes occur must therefore be governed by the 138 day half-life of ^{210}Po. To get ^{218}Po and ^{214}Po radiohalos these processes would have to have occurred even faster. (Snelling 2005a)

If the U and Po radiohalos both formed during the 6–10 days while the granite plutons cooled during the Flood, then this implies 100 million years' worth of accelerated ^{238}U decay occurred in a time frame of a few days. Thus the U-Pb isotopic systematics within the zircons in these granite plutons are definitely not providing absolute "ages" as conventionally interpreted.

Field and Laboratory Methods

Mapping and sampling

July–September 1974 was spent geological mapping an area of almost 95 km^2 (almost 37 sq. mi.) straddling the margins of the Bathurst Granite and the adjoining fossil-bearing sedimentary host rocks (figs. 2 and 6). The study area embraces the villages of Sodwalls and Tarana in the southeastern and southwestern corners respectively, and the village of Meadow Flat in the northwest corner (fig. 4). Access to much of the area was facilitated by the major western railroad from Sydney, and the Great Western Highway traverses across the northern boundary and passes through Meadow Flat.

Mapping was accomplished by using 1964 air-photo coverage of the Bathurst district (Bathurst Run Numbers 10 and 11, Photo Numbers 5162-5167

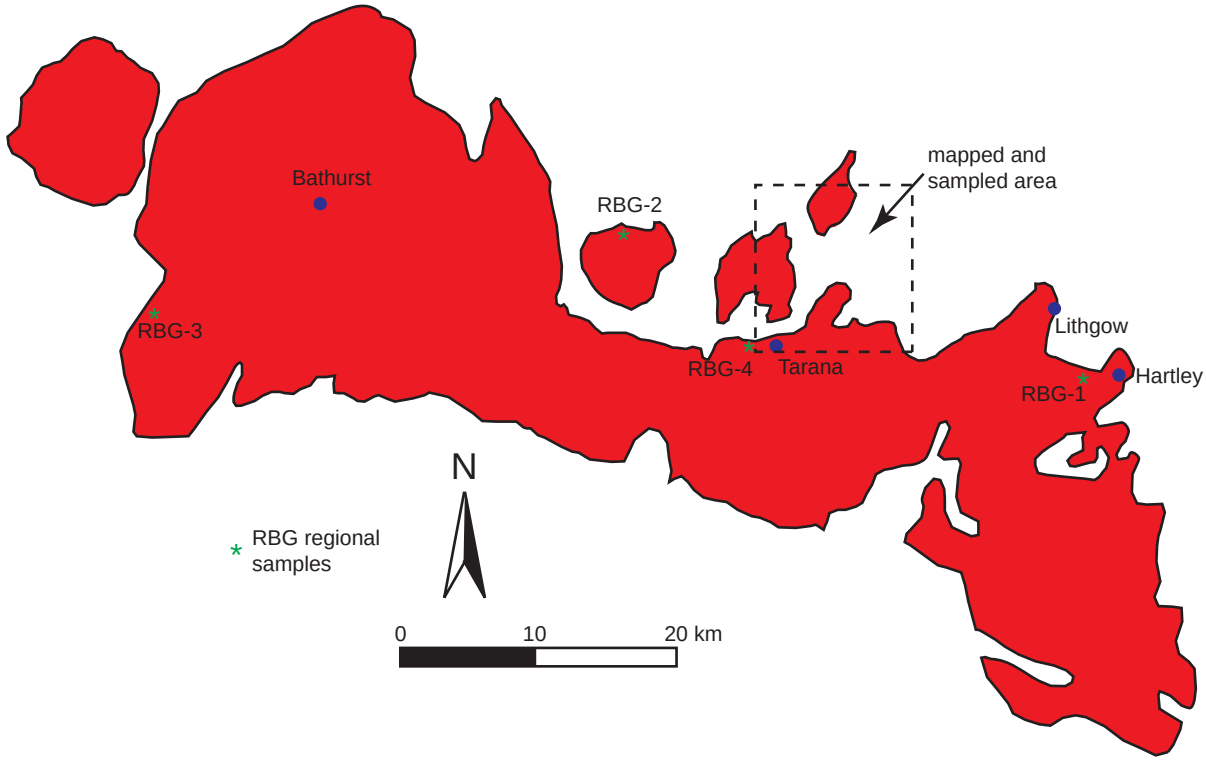

Fig. 6. Regional outline of the Bathurst Batholith, showing the location of the area mapped and sampled in July–September 1974 and locations of the regional samples collected in July 1999.

and 5057-5062, respectively). Pairs of aerial photos were closely examined through a stereoscopic viewer and the tentative boundaries between various rock units were annotated on the photos, along with the locations of outcrops. A tentative geologic map was then compiled from this air-photo interpretation by transferring it to a composite overlay. The geological map produced (fig. 4) was originally at the air-photo scale of 1:38,000.

This tentative geological map was field checked along the boundaries between the different strata, recording geologic details at different outcrops. Traverses were done on foot along the railroad, along creeks and their tributaries, and across ridges and hills. Various outcrops were appropriately sampled and significant features photographed, with the locations of these being carefully recorded on the geological map being compiled. Samples were named and numbered appropriately according to the various rock types. Where appropriate, strike and dip measurements were made on bedding planes in the outcrops of the sedimentary rock units, and such details were also recorded on the geological map being compiled.

Further fieldwork was undertaken in the region in July 1999. The aim was to give a regional perspective to the previously mapped and sampled area, which represented only a small fraction of the margins of the Bathurst Batholith (fig. 6). Several outcrops were sampled along the highways and minor roads that skirt around and cross the batholith, the chosen samples being representative of the margins of the batholith for comparison with similar samples in the earlier intensely mapped area.

Chemical analyses

Seven samples collected during the 1974 fieldwork were selected for further chemical analyses. These included two from the Bathurst Granite, three from the Evans Crown dike (one from a feeder dike, one from the coarse-grained phase, and one from the chilled margin), and two samples of porphyry dikes that cross-cut both the Bathurst Granite and the Evans Crown dike. These samples were sent to the Perth (Western Australia) laboratories of Associated Laboratories of Australia Pty Ltd for whole-rock analyses.

Laboratory methods

Samples were crushed and pulverized. The following methods were then used to analyze the chemical compositions of these rocks:

1. X-ray Fluorescence (XRF) fusion analysis was used to determine Si, Al, Fe, Ti, Ca, and K concentrations, as well as the loss on ignition ($H_2O\pm$). To accomplish this, the pulverized samples were heated in a platinum crucible to 1000°C, fused with a lithium tetraborate based flux, and quenched quickly. A counting precision of ±2% was obtained by accumulating more than 2500 counts per element peak. Detection limits were rather less than 500 ppm, depending on the matrix.
2. Atomic Absorption Spectroscopy (AAS) was used to analyze for Mg, Mn, Na, Cu, and Mo following total acid attack of the pulverized samples. While Mg and Mn were included in the XRF fusion determination, the AAS method allows a 100-fold reduction in the detection limit. Precision, based on the measuring of light intensities, was better than 5%. Detection limits were all routinely 5 ppm.
3. X-ray Fluorescence (XRF) pressed powder pellet analysis was used to determine S concentrations, assuming levels not much higher than 1%. Precision depended to a large extent on particle size, but a precision of ±5% or ±50 ppm has been consistently demonstrated at this laboratory.

Once all the results were obtained the weight percents of the major elements were calculated, followed by distribution of oxygen proportionally to the various oxides in order to recalculate the oxide percentages. Trace elements were reported as ppm concentrations.

Samples selected for radiohalos counting were thin-sectioned in order to characterize the mineralogy and textures of the different rock types, particularly the granites from the main batholith mass and satellite stocks, the granitic rocks from the dikes, and the host rocks adjoining the margins of the granite where metamorphism had occurred. Furthermore, an accurate assessment of the mineral content of several samples of the Bathurst Granite and the Evans Crown dike were obtained by point counting of thin sections for statistical analyses.

Counting of radiohalos

Twenty-four samples of granitic rocks were selected from those collected in 1974, and four granite samples collected in 1999. Of these 28 samples, twelve were of the Bathurst Granite, eight were from the Evans Crown dike (seven of coarse-grained granitic dike rock and one from the dike's chilled margin), four were from granitic dikes intruded across the Bathurst Granite, two were from granitic dikes intruding through the Evans Crown dike, and two were from granitic dikes cross-cutting the host sedimentary rocks.

Portions of the 28 samples were crushed to liberate the biotite grains. Biotite flakes were then handpicked with tweezers from each crushed sample and placed on a piece of Scotch tape™ fixed to the flat surface of a laminated board on a laboratory table with its adhesive side up. Once numerous biotite

Fig. 7. Panoramic view looking southwest and west from the summit of Mt. Lambie (from Snelling 1974). To the left in the distance the Evans Crown dike is easily recognized with its prominent granite tors on the middle. Moving right the topographic hollow of the Solitary Creek valley is seen, as marked on Fig. 4. The Evans Crown dike crosses that valley and forms the ridge (Evans Crown) in the middle of the view (center and right). The Deadman's Creek valley separates the latter ridge and Mt. Lambie (just beyond the foreground). The Tarana Range looms in the background (middle right).

flakes had been mounted on the adhesive side of this piece of tape, a fresh piece of Scotch tape™ was placed over them and firmly pressed along its length so as to ensure the two pieces were stuck together with the biotite flakes firmly wedged between them. The upper piece of tape was then peeled back in order to pull apart the sheets composing the biotite flakes, and this piece of tape with thin biotite sheets adhering to it was then placed over a standard glass microscope slide so that the adhesive side and the thin mica flakes adhered to it. This procedure was repeated with another piece of Scotch tape™ placed over the original tape and biotite flakes affixed to the board, the adhering biotite flakes being progressively pulled apart and transferred to microscope sides. As necessary, further handpicked biotite flakes were added to replace those fully pulled apart. In this way tens of microscope slides were prepared for each sample, each with many (at least 20) thin biotite flakes mounted on it. This is similar to the method pioneered by Gentry (1988). A minimum of 50 microscope slides was prepared for each sample (at least 1000 biotite flakes) to ensure good representative sampling statistics.

Each slide for each sample was then carefully examined under a petrological microscope in plane polarized light and all radiohalos present were identified, noting any relationships between the different radiohalo types and any unusual features. The numbers of each type of radiohalo in each slide were counted by progressively moving the slide backwards and forwards across the field of view, and the numbers for each slide were then tallied and tabulated for each sample.

Results

Mapping and sampling

The geological map resulting from the intense fieldwork is shown in Fig. 4 (Snelling 1974). Marked on the map are the interpreted boundaries between the various outcropping rock units in the area, the creek drainages, the villages, the major roads, and the railroad. The strike and dip measurements of the bedding in the host sedimentary units are recorded on the map in the locations they were obtained, and the numbered black dots represent the sample collection sites. Only those samples used in this radiohalos study are marked on the map. And around the borders of the map not only are the longitude east and latitude south coordinates marked, but there is also a one kilometer by one kilometer grid coordinates system marked and annotated for ease of referencing map locations.

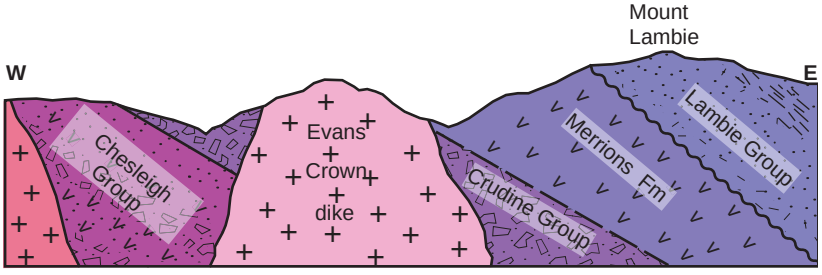

Fig. 8. The local composite stratigraphic cross-section, drawn approximately east-west through the summit of Mt. Lambie (from Snelling 1974).

Fig. 9. View of the Solitary Creek valley with the railroad from Sydney west to Parkes on the extreme right (from Snelling 1974). Bald Ridge (marked on fig. 4) lies in the center of the view, with the Evans Crown dike cropping out along the ridge to the left. In the railroad cuts to the immediate right of Bald Ridge the Evans Crown dike is found to split into a multitude of coalescing smaller dikes. The margins of the Bathurst Granite occupy the low-lying land along Solitary Creek because the granite is more weathered.

The host sedimentary rocks and stratigraphic sequences and relationships are shown in Fig. 3. Because they have been regionally metamorphosed, they are more resistant to weathering and erosion, so they form the higher ground in the panoramic view in Fig. 7. This view is looking west and southwest from the summit of Mt. Lambie, at 1284 m (4213 ft.) the highest point in the map area (fig. 4). The next ridge to the west (center and right in fig. 7) is the Evans Crown dike. These topographic variations according to the rock types can also be seen in the geological cross-section in Fig. 8, which cuts approximately east-west across Fig. 4 through the summit of Mt. Lambie. Because the Bathurst Granite is more weathered, it occupies the lower ground along Solitary Creek in the southern portion of the map area (fig. 4), as observed in Figs. 7 and 9.

Adjacent to the margins of the Bathurst Granite in the west and north of the map area are outlying stocks of the same granite—the Eusdah and Meadow Flat stocks respectively (figs. 4 and 10). Cross-cutting the margin of the Bathurst Granite near Tarana and then through the surrounding host sedimentary rocks roughly northwards to form Bald Ridge (figs. 4 and 9) and Evans Crown (fig. 7) is the granitic Evans Crown dike (fig. 11), which is estimated to be 12.8 km (8 mi.) long and often 0.8 km (0.5 mi.) wide. In the railroad cuts beside Solitary Creek to the immediate south of Bald Ridge within the Bathurst Granite the Evans Crown dike was found to split into multiple, coalescing smaller dikes. In the same area several granitic (acid) dikes are found within the Evans Crown dike, following and paralleling jointing. A few basaltic (basic) dikes (fig. 12) and numerous minor granitic dikes (similar to those that are within the Evans Crown dike) also cut across the margins of the Bathurst Granite, also following and paralleling jointing, and extend out into the surrounding host sedimentary strata (fig. 13). Good exposures of these dikes are seen in the many railroad cuts between

Fig. 10. Prominent outcrop of the Bathurst Granite in the Meadow Flat stock at grid reference 928693 in Fig. 4 (from Snelling 1974).

Fig. 11. Outcrop of the granitic Evans Crown dike at grid reference 939636 in Fig. 4 (from Snelling 1974). Mineral variations within this dike parallel the jointing, which can be seen prominently running through the crest of the outcrop.

Fig. 12. A basaltic (basic) dike cutting across the Bathurst granite in a railroad cut at grid reference 948587 in Fig. 4 (from Snelling 1974). Notice the parallel jointing in both the dike and the granite, due to the basaltic magma having intruded along the jointing in the granite.

Sodwalls and Tarana (fig. 4). Up to 45 m (about 150 ft.) wide, these granitic dikes have the same mineral composition as both the Bathurst Granite and the Evans Crown dike, often with the same porphyritic texture.

Fig. 13. View of the weathered Bathurst Granite along the Solitary Creek valley at grid reference 958584 in Fig. 4 (from Snelling 1974), showing the linear outcrops of cross-cutting dikes which can be traced across the fields.

The regional context of the mapped area in relation to the whole Bathurst Batholith is shown in Fig. 6. The sites from which the regional samples of the Bathurst Granite were collected are marked. These chosen samples were representative of the batholith and very similar in appearance and composition to the Bathurst Granite in the mapped area.

Chemical analyses

The whole-rock chemical analyses for the selected granitic rocks are listed in Table 1. Included in this table is a sample of the Bathurst Granite from the Sodwalls area (sample 2) whose chemical analysis was reported by Joplin (1963).

Photomicrographs representative of some of the samples of the Bathurst Granite, the Evans Crown dike and the minor granitic dikes are provided in Fig. 14. The mineral contents of selected samples of the Bathurst Granite and the Evans Crown dike obtained by point counting of thin sections, the modal analyses, are listed in Table 2.

Counting of radiohalos

Photomicrographs of some representative radiohalos are shown in Fig. 15. The statistics of the counted radiohalos in the 28 chosen granitic samples are listed in Table 3. The number of radiohalos per slide was calculated by adding up the total number of all radiohalos found in each sample, divided by the number of slides made and viewed for counting of radiohalos. The number of Po radiohalos per slide was calculated in a similar way, except it was the total number of Po radiohalos divided by the number of slides examined for that sample. And finally, the ratio in the last column was calculated by taking the number of ^{210}Po radiohalos and dividing by the number of ^{238}U halos.

Discussion

Results of the present study

In the mapped area there is a definite sequence for the formation of the granitic rocks. The fossil-bearing sedimentary rocks were first intruded by the major pluton of the Bathurst Granite. Fig. 16 shows the contact of the Bathurst Granite (right) with the host fossil-bearing Lambie Group sedimentary strata in a railroad cut at grid reference 993589 in Fig. 4 (from Snelling 1974). Notice the vein-like apothyses of granite protruding into the sedimentary strata from the granite to the left of the line of contact. Also notice that the bedding of the sedimentary layers has been disturbed near the contact. Both these observations indicate the granite had the constituency of a hot magma that flowed as it forced its way up and into the host sedimentary strata, rather than being a cold, solid body that was tectonically emplaced.

Table 1. Whole-rock chemical analyses, expressed in oxide percent, of Bathurst Granite and granitic dikes of the Tarana-Sodwalls area (from Snelling 1974).

	1	2	3	4	5	6	7	8
SiO_2	66.73%	69.36%	72.65%	73.75%	73.96%	74.94%	76.96%	77.51%
Al_2O_3	15.32%	13.46%	13.36%	13.16%	13.74%	12.86%	12.65%	12.25%
Fe_2O_3	3.95%	3.00%	2.05%	1.68%	1.51%	1.57%	1.09%	0.86%
FeO		0.81%						
MgO	0.42%	0.86%	0.24%	0.10%	0.11%	0.07%	0.04%	0.02%
CaO	3.29%	2.20%	1.27%	0.93%	0.81%	0.43%	0.44%	0.30%
Na_2O	3.22%	3.78%	3.36%	3.73%	3.88%	3.49%	2.08%	4.03%
K_2O	4.75%	4.29%	4.97%	5.32%	5.44%	5.35%	4.79%	4.68%
$H_2O^{\pm}$	0.96&	1.82%	1.74%	1.09%	0.81%	0.69%	1.10%	0.67%
TiO_2	0.64%	0.50%	0.34%	0.28%	0.27%	0.25%	0.07%	0.05%
MnO	0.04%	0.14%	0.03%	0.03%	0.03%	0.02%	0.03%	0.03%
Total	99.32%	100.22%	100.01%	100.07%	101.56%	99.67%	99.25%	100.40%
S	93 ppm	—	61 ppm	86 ppm	54 ppm	15 ppm	15 ppm	20 ppm
Cu	20 ppm	—	15 ppm	15 ppm	15 ppm	177 ppm	58 ppm	27 ppm
Mo	5 ppm	—	8 ppm	2 ppm	2 ppm	4 ppm	2 ppm	5 ppm

1. Granite, Sodwalls. Analyst—Associated Laboratories of Australia
2. Granite, Sodwalls. Analyst—W. G. Stone (Joplin 1963)
3. Porphyry dike, between Sodwalls and Tarana. Analyst—Associated Laboratories of Australia
4. Dikes of the Evans Crown dike Railway Cuttings. Analyst—Associated Laboratories of Australia
5. Chilled Margin, Evans Crown dike. Analyst—Associated Laboratories of Australia
6. Coarse-grained phase, Evans Crown dike. Analyst—Associated Laboratories of Australia
7. Porphyry dike near Sodwalls. Analyst—Associated Laboratories of Australia
8. Granite, Meadow Flat. Analyst—Associated Laboratories of Australia

Further observations to answer this question of whether the granite was hot or cold when intruded are readily available. The granite at the contact and in the apothyses in Fig. 16 is coarse-grained and is the same as the granite outcropping elsewhere in the pluton, so the intruding granite body appears to have been at a uniform temperature. If the pluton had been tectonically emplaced there should be evidence in the contact zone either of melting and recrystallization or of mechanical crushing of the granite. If melting and recrystallization had occurred, then the granite at the contact with the sedimentary strata and in the apothyses could be expected to be of a noticeably different grain size than the granite in the main body, contrary to what is observed. Alternately, if any mechanical crushing had occurred at the margin of the granite body, then the granite and the host sedimentary layers at the contact should exhibit signs of mylonitization, which is not evident. Also, no vein-like apothyses would be expected, as those indicate fluid flow, and not mechanical crushing.

Additionally the hot granite intrusion would have impacted the adjacent host fossil-bearing sedimentary strata, creating the observable contact metamorphic aureole. As already noted (Fig. 16), it is evident that the sedimentary layering very close to the granite contact has been disturbed, not crushed, likely both by intrusion of the main granite body and of the apothyses. This would have been due to the mechanics of fluid flow of a hot magma, rather than tectonic emplacement of a cold body. Nevertheless, the definitive observation that is consistent with intrusion of a hot granitic magma is the contact metamorphism of the host sedimentary strata adjacent to the granite margin.

Both Mackay (1959) and Snelling (1974) cataloged the contact metamorphic mineral assemblages in the aureole adjacent to the margins of the Bathurst Granite in the Sodwalls-Tarana area (fig. 4). These mineral assemblages are summarized in the ACF-A′KF diagrams in Fig. 17. The depicted mineral assemblages of the albite-epidote-hornfels facies are found in the host sedimentary rocks in the outer fringes of the contact aureole where the temperatures of contact metamorphism were very low. Furthermore, many of these same minerals characterize the assemblages typical of the greenschist facies produced by the regional burial metamorphism of these sedimentary strata. However, the mineral assemblages of the hornblende-hornfels facies in the aureole closer to the contact with the Bathurst Granite stand out in clear contrast to the regional burial metamorphism of the surrounding host sedimentary strata. This facies embraces the majority of rocks that form the obvious contact aureole. It is also significant that sillimanite, which is characteristic of the even higher temperature pyroxene-hornfels facies, is not present in the aureole even closer to the contact, but is found in the granite right at the boundary (Snelling 1974).

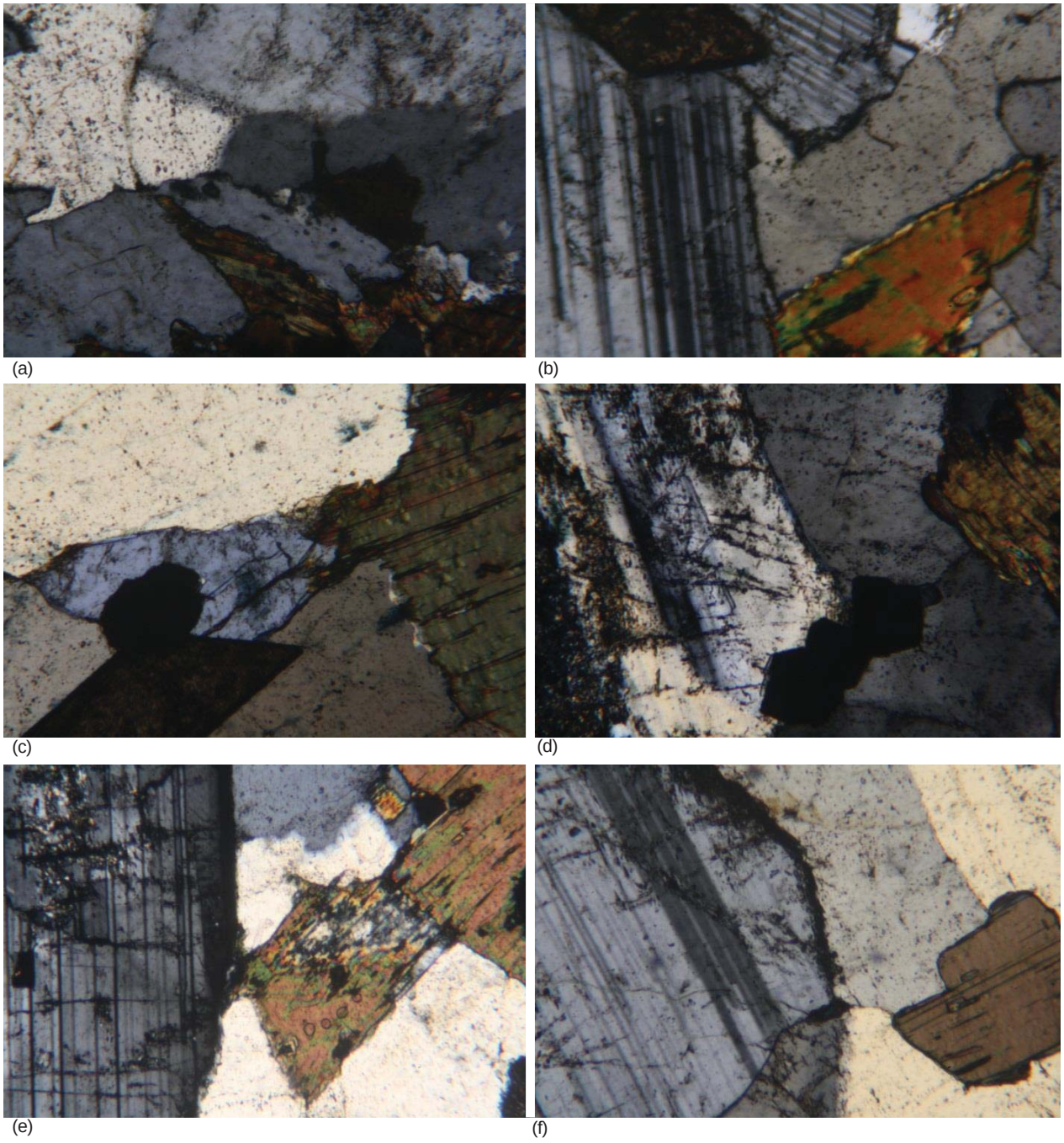

Fig. 14. Photomicrographs representative of some of the samples of the Bathurst Granite, Evans Crown dike, and granitic dikes intruding them used in this study, as seen under the microscope. Their locations are plotted on Fig. 4. All photomicrographs are at the same scale (20× or 1 mm = 40μm) and the granites are as viewed under crossed polarized light.
Bathurst Granite:–
(a) Sample RBG-4: K-feldspar (plain mid gray), quartz (light color), biotite (bright colors partly extinguished).
(b) Sample ASI-32: plagioclase (striped gray), K-feldspar (plain dull gray), biotite (bright colors), sphene (prismatic crystal), quartz (light color).
(c) Sample ASI-32: quartz (light yellowish color), biotite (bright colors partly extinguished), sphene (prismatic crystal), K-feldspar (plain mid and dull gray), magnetite (black).
(d) Sample ASI-31: plagioclase (striped gray), K-feldspar (plain mid gray), biotite (bright colors), magnetite (black).
(e) Sample ASI-23: plagioclase (striped gray), quartz (light yellowish color), biotite (bright colors), K-feldspar (plain mid gray).
(f) Sample ASI-23: plagioclase (striped gray), quartz (light yellowish color), K-feldspar (plain mid gray), biotite (bright colors).

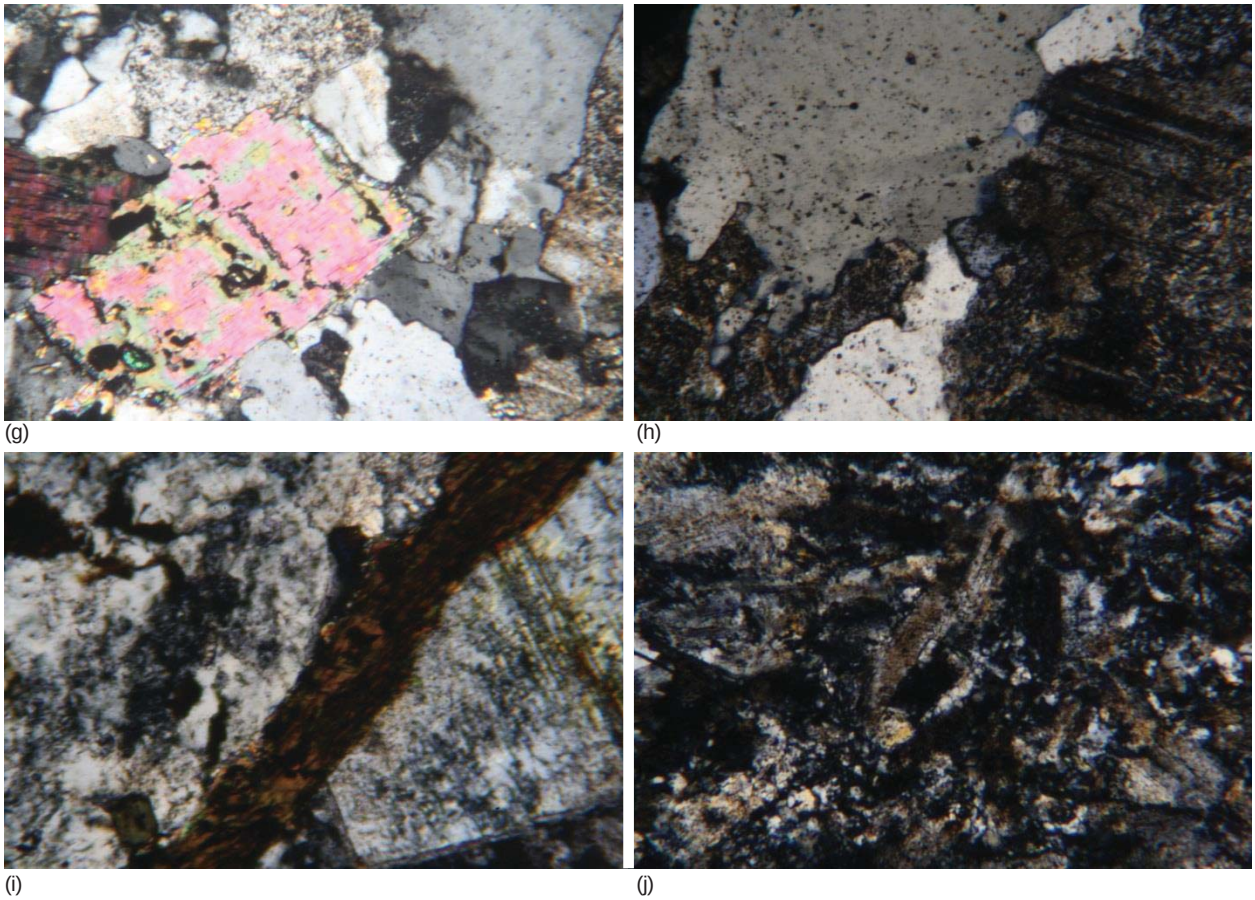

Fig. 14 (continued). Evans Crown dike:–
(g) Sample ASI-46: biotite (bright colors), K-feldspar (plain mid gray), plagioclase (speckled gray due to alteration to sericite).
(h) Sample ASI-46: K-feldspar (plain mid gray), plagioclase (remnant striping and speckled gray due to alteration to sericite).
(i) Sample ASI-17: biotite (dark brown due to alteration), altered plagioclase (right, striped speckled mid gray) and K-feldspar (left, speckled mid gray).
(j) Sample ASI-17: altered plagioclase and K-feldspar (speckled mid gray and black), minor quartz (light yellowish color).

The pressure-temperature (P-T) conditions in the contact aureole can be determined by the experimental calibration curves for the mineral reactions. Fig. 18 depicts the P-T fields of these facies of contact metamorphism (Turner 1968). The position of the minimum melting curve for quartz-orthoclase-albite (Qz-Or-Ab) implies the highest temperature at the least pressure (that is, the shallowest depth) at which the hornblende-hornfels facies would be produced in this aureole against the molten Bathurst Granite is 700°C and 2 kb pressure, approximately equivalent to a depth of less than 5 km (3 mi.) (Bucher and Fry 2002). Confirmation that the depth of granite emplacement was shallow is indicated by the observations of jointing and flow banding in the granite consistent with those outcrops near the roof of the pluton (Snelling 1974), and confirmed by measurements of the stratigraphic thicknesses above the granite. Independent confirmation that the granite would have been molten at 700°C (or more) is consistent with experimental work on granite formation (Johannes and Holtz 1996; Tuttle and Bowen 1958).

Field relationships clearly indicate that the Evans Crown dike intruded into a major fracture through the Bathurst Granite and also penetrated across into the surrounding sedimentary strata. The dike's central portions are coarse and even-grained like the Bathurst Granite, but the margins are chilled against the host granite. These relations indicate the dike intruded as a hot granitic magma similar to that of the Bathurst Granite (and likely even from the same magma source). Other observations indicate the Bathurst Granite had cooled considerably prior to this dike's intrusion. Some of the chilled margins in the dike exhibit pronounced flow-banding texture parallel to the contact (Snelling 1974). Furthermore, the development of graphic quartz-feldspar intergrowths, myrmekitic outgrowths and reaction-rimmed grains in the dike also suggest the Bathurst Granite had cooled prior to the dike's intrusion.

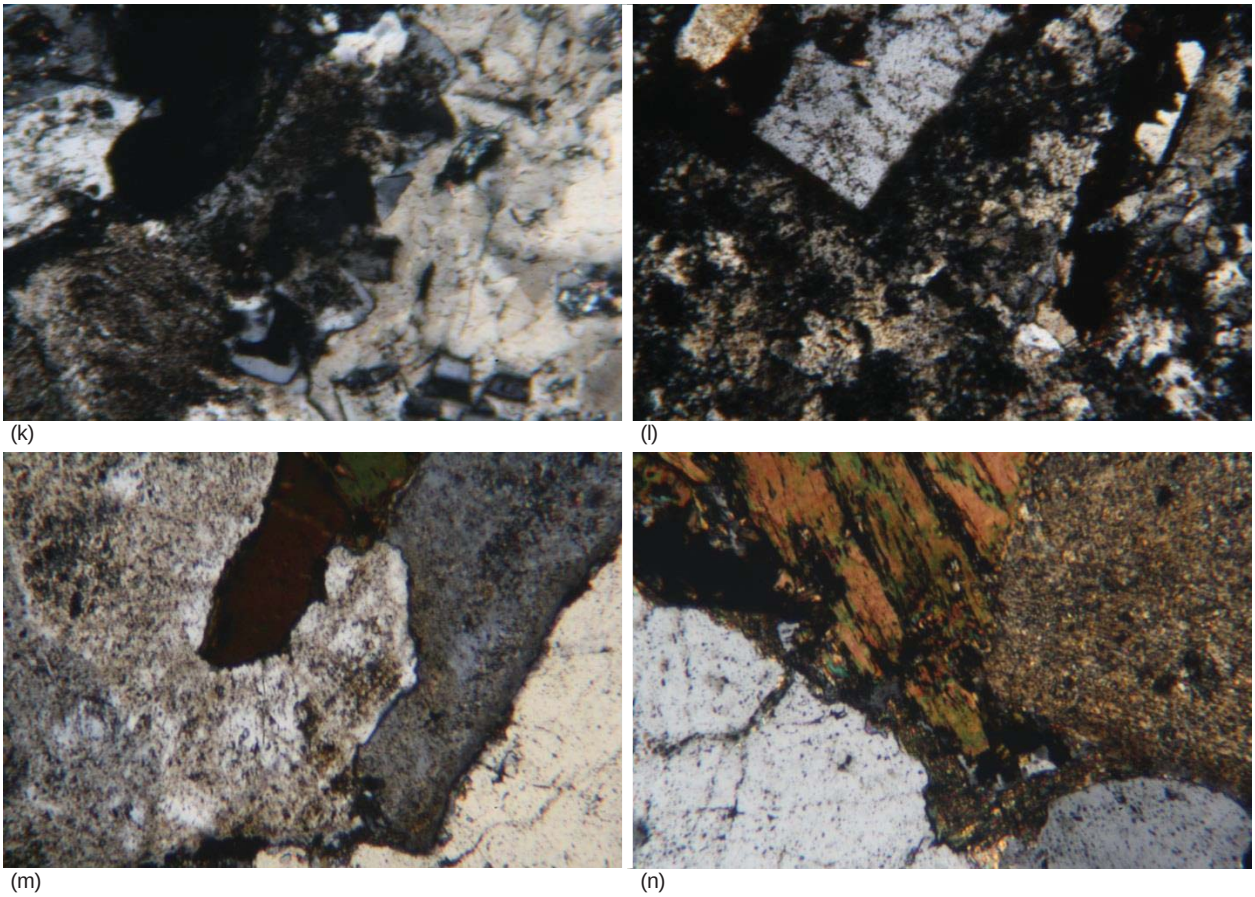

Fig. 14 (continued). Granite dikes:–
(k) Sample ASI-57: minor quartz (light yellowish color), altered plagioclase (crystal shape right, speckled mid gray) and K-feldspar (speckled mid gray and black).
(l) Sample ASI-109: minor quartz (light yellowish color), altered plagioclase (crystal shape top, speckled mid gray) and K-feldspar (speckled mid gray and black).
(m) Sample ASI-110: plagioclase (speckled gray and brown due to alteration to sericite and iron oxides), K-feldspar (plain mid gray), biotite (bright colors).
(n) Sample ASI-110: plagioclase (speckled gray and brown due to alteration to sericite and iron oxides), biotite (bright colors), K-feldspar (plain mid gray).

Table 2. Modal analyses of the mineral contents of the Bathurst Granite and the Evans Crown dike of the Tarana-Sodwalls area obtained by point counting of thin sections.

Mineral	1	2	3	4	5	6	7	8
Quartz	29.3%	27.6%	28.7%	27.3%	26.2%	26.9%	27.3%	28.1%
Orthoclase	22.5%	21.4%	31.3%	31.5%	27.5%	31.6%	32.7%	33.9%
Plagioclase	42.1%	41.0%	32.8%	33.2%	43.6%	40.8%	39.1%	36.5%
Hornblende	5.0%	8.6%	5.5%	6.2%	—	—	—	—
Biotite					2.7%	0.6%	0.9%	1.5%
Opaques	0.5%	0.9%	0.8%	1.3%	(0.01%)	(0.01%)	(0.02%)	(0.03%)
Sphene	0.6%	1.5%	0.9%	0.5%	—	—	—	—

1. Bathurst Granite, Sodwalls. (Mackay 1959)
2. Bathurst Granite, Sodwalls. (Mackay 1959)
3. Bathurst Granite, Sodwalls.
4. Bathurst Granite, Sodwalls.
5. Evans Crown dike. (Mackay 1959)
6. Evans Crown dike. (Mackay 1959)
7. Evans Crown dike.
8. Evans Crown dike.

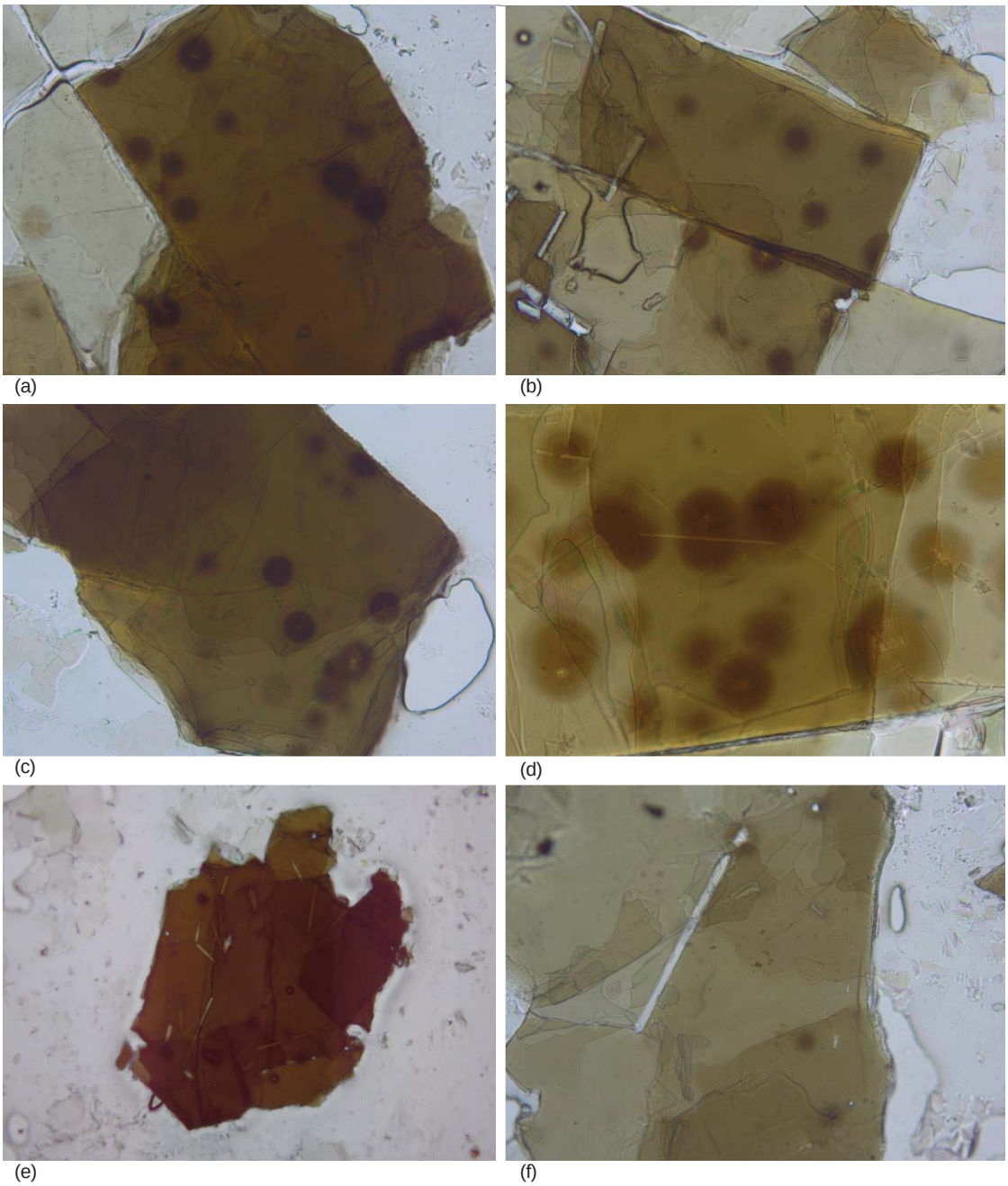

Fig. 15. Photomicrographs of some representative ^{238}U and ^{210}Po radiohalos in biotite flakes in samples of the Bathurst Granite, Evans Crown dike, and granitic dikes intruding them, as seen under the microscope. All the biotite grains are as viewed in plane polarized light, and the scale bars are all 50 µm (microns) long. Bathurst Granite: samples ASI-32 (a), (b) (c) and (d); ASI-23 (e) and (f).

Following intrusion of the Evans Crown dike, residual granitic magma intruded as smaller dikes that cut across the Bathurst Granite. These dikes follow joints and fractures within and parallel to the Evans Crown dike, and they also continue out into and across the host sedimentary strata. Both reaction textures and mineral intergrowths within these granitic dikes suggest the phenocrysts crystallized prior to the injection of the dikes into the Bathurst Granite, and also across the Evans Crown dike (Snelling 1974). Alteration zones marginal to the sharp contacts of the dikes with the wall-rocks indicate the magma was still hot when injected, and the dikes are frequently flow-banded parallel to these contacts (fig. 19).

Whole-rock chemical analyses of the granitic rocks are listed in Table 1 in order of increasing silica (SiO_2) content. Note that the Bathurst Granite samples have the lowest silica content, and that in the later dike phases (both the Evans Crown dike and the smaller dikes that intrude it and the Bathurst Granite) the silica content is increased. This silica trend somewhat

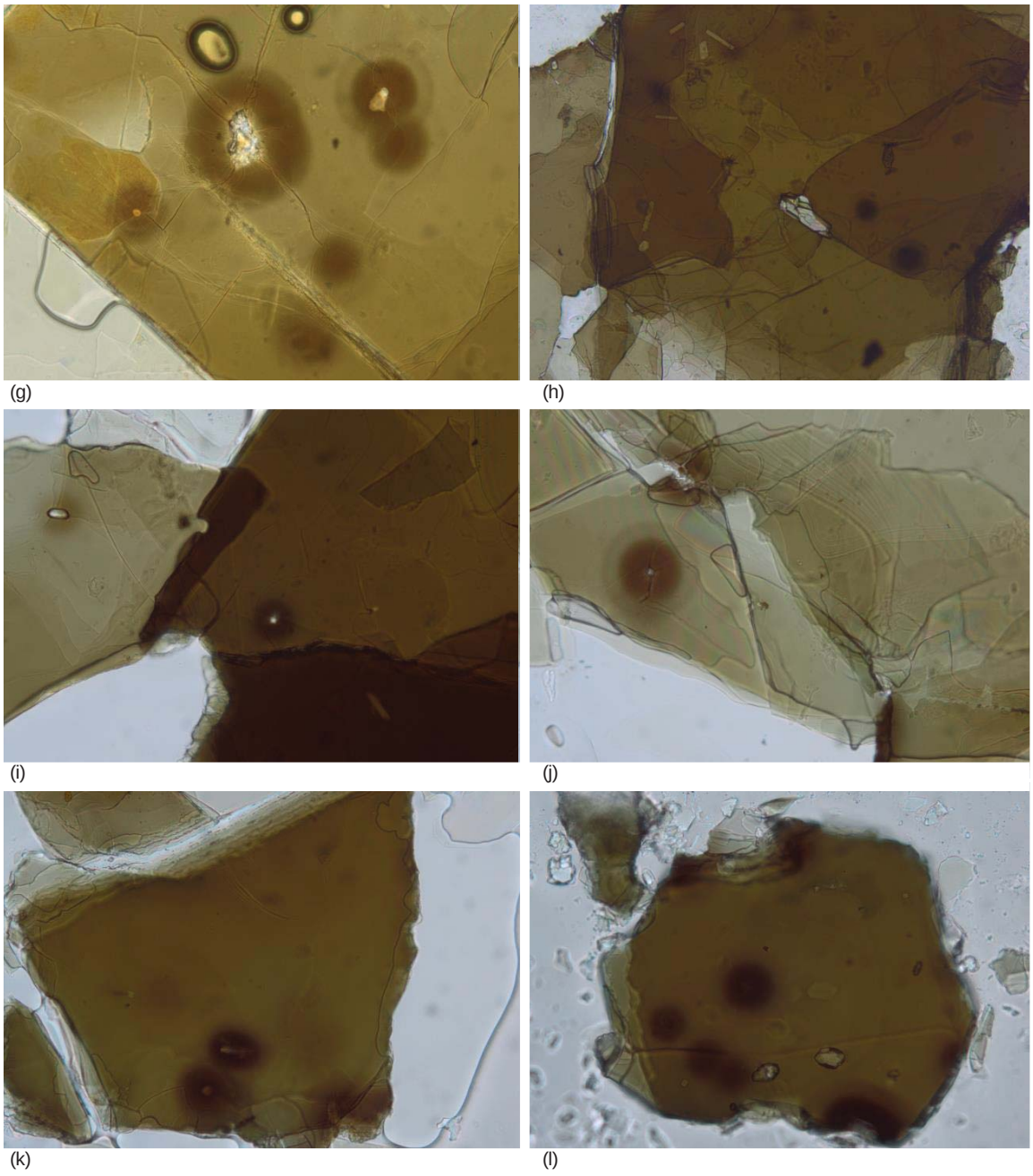

Fig.15 (continued). Photomicrographs of some representative ^{238}U and ^{210}Po radiohalos in biotite flakes in samples of the Bathurst Granite, Evans Crown dike, and granitic dikes intruding them, as seen under the microscope. All the biotite grains are as viewed in plane polarized light, and the scale bars are all 50 µm (microns) long. Bathurst Granite: samples ASI-31 (g); RBG-3 (h) and (i); ASI-68 (j) and (k); and ASI-37 (l).

parallels the time sequence of intrusion, which is consistent with the interpretation that later granitic dike phases were derived from residual magma of the Bathurst Granite. This relationship is well-recognized and characterized in the literature (Hall 1996). The exception is the Meadow Flat Granite in the satellite stock, north of the mapped area (fig. 4), which is lithologically similar to the Bathurst Granite, but has the highest silica content of the samples (table 1). This may suggest that because the stock was intruded peripherally to the main body of the batholith, it intruded laterally as a residual magma from the main Bathurst Granite pluton.

The pioneering experimental work of Tuttle and Bowen (1958) led to the development of graphical schemes for the classification of granitic rocks based on both modal and normative analyses. Modal analyses are obtained by direct point counting of the observed mineral contents of the rocks in thin sections, whereas normative analyses rely on calculating the ideal mineral contents from the oxides obtained in whole-rock chemical analyses. Once obtained,

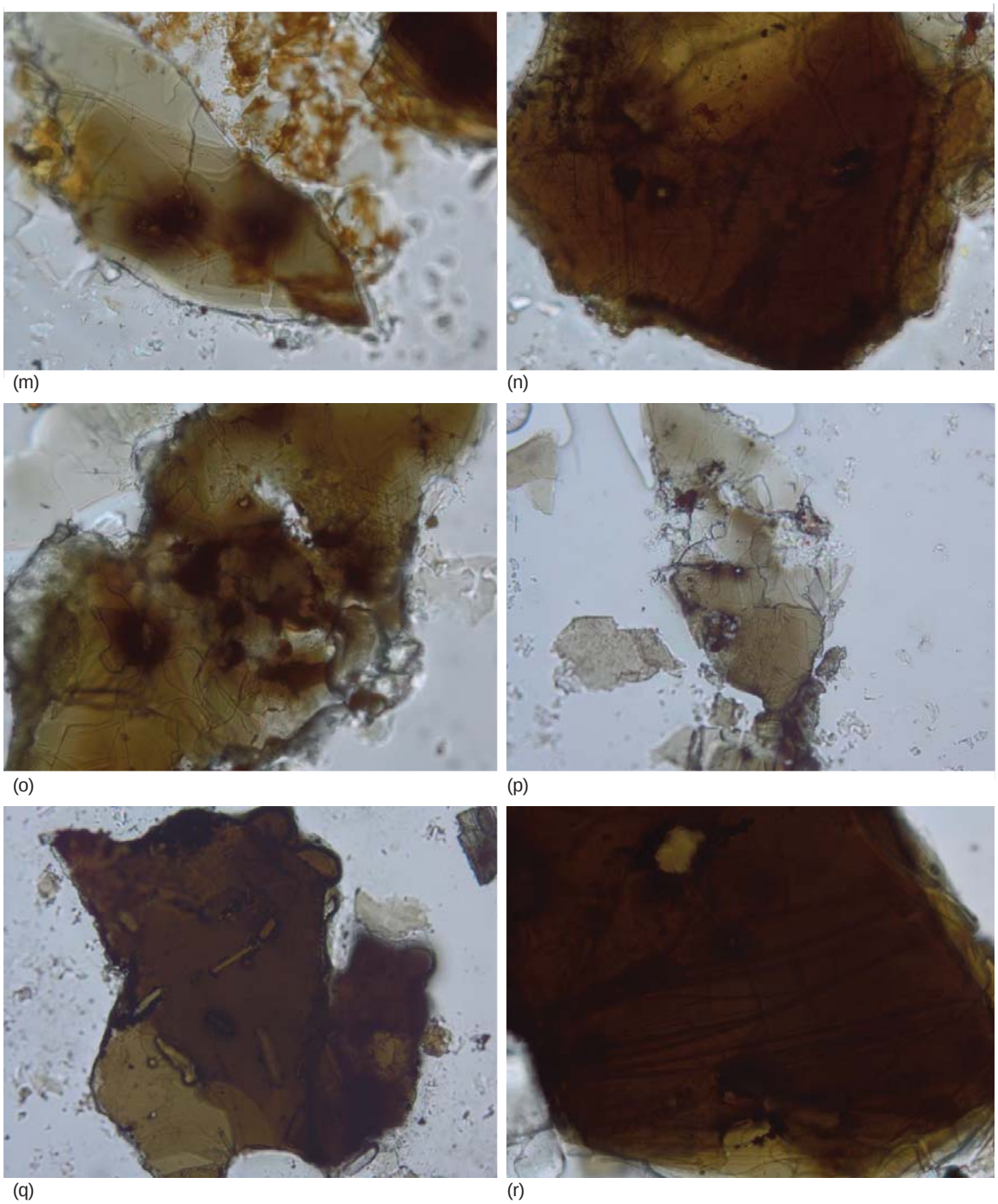

Fig.15 (continued). Photomicrographs of some representative ^{238}U and ^{210}Po radiohalos in biotite flakes in samples of the Bathurst Granite, Evans Crown dike, and granitic dikes intruding them, as seen under the microscope. All the biotite grains are as viewed in plane polarized light, and the scale bars are all 50 µm (microns) long. Evans Crown dike: samples ASI-46 (m); and ASI-44 (n). Granitic dike intruding Bathurst Granite: sample ASI-57 (o) and (p). Granitic dike intruding Evans Crown Dike: sample ASI-110 (q) and (r).

the modal and normative analyses were recast or normalized so that the three components quartz, orthoclase and plagioclase, and quartz, orthoclase and albite respectively totalled 100% for each rock. These were then plotted on triangular composition diagrams with the respective minerals at their apices (figs. 20 and 21). The surprising results were that both schemes plotted around the same point, the point representing one third of each mineral component, and corresponded exactly with the results of their laboratory work on artificial silicate systems.

Tuttle (1955), Tuttle and Bowen (1958) and Johannes and Holtz (1996) discuss the magmatic origin of granite based on experimental work on artificial silicate systems. Tuttle and Bowen (1958) demonstrated that the path of crystallization in the

Table 3. Radiohalos count statistics for samples of the Bathurst Granite and granitic dikes of the Tarana-Sodwalls area.

Rock Unit	Location	Sample Number	Number of Slides	Numbers of Radiohalos					Number of Radiohalos per Slide	Number of Po Radiohalos per Slide	Ratio $^{210}Po:^{238}U$
				^{210}Po	^{214}Po	^{218}Po	^{238}U	^{232}Th			
Bathurst Granite	Hartley	RBG-1	51	45	—	—	3	—	0.94	0.88	15:!
	Yetholme	RBG-2	50	39	—	—	3	—	0.84	0.78	13:1
	Newbridge	RBG-3	50	206	—	7	54	—	5.34	4.26	3.8:1
	Tarana	RBG-4	51	2270	23	520	1694	31	88.98	55.16	1.3:1
	Sodwalls	ASI-23	50	102	—	—	1	—	2.06	2.04	102:1
		ASI-31	50	142	—	—	5	—	2.94	2.84	28.4:1
		ASI-32	50	181	—	—	100	—	5.62	3.62	1.8:1
		ASI-55	50	58	—	—	2	—	1.20	1.16	27.5:1
	Meadow Flat	ASI-37	50	220	—	—	81	—	6.02	4.40	27:1
		ASI-38	50	13	—	—	3	—	0.32	0.26	4.3:1
		ASI-66	50	60	1	—	18	—	1.58	1.22	3.3:1
		ASI-68	50	102	—	—	29	—	2.62	2.04	3.5:1
Evans Crown dike	coarse-grained	ASI-21	50	7	—	—	—	—	0.14	0.14	—
		ASI-22	50	11	—	—	—	—	0.22	0.22	—
		ASI-44	50	74	—	—	9	—	1.66	1.48	8.2:1
		ASI-46	50	90	—	—	6	—	1.92	1.80	15:1
		ASI-51	50	21	—	—	12	—	0.66	0.42	1.8:1
		ASI-58	50	1	—	—	5	—	0.12	0.02	0.2:1
		ASI-59	50	22	—	—	2	—	0.48	0.44	11:1
	chilled margin	ASI-17	50	1	—	—	—	—	0.02	0.02	—
Dikes	intruding Bathurst Granite	ASI-07	50	—	—	—	—	—	—	—	—
		ASI-24	50	—	—	—	—	—	—	—	—
		ASI-34	50	—	—	—	—	—	—	—	—
		ASI-57	50	5	—	—	—	—	0.10	0.10	—
Dikes	intruding Evans Crown dike	ASI-109	50	—	—	—	—	—	—	—	—
		ASI-110	50	7	—	—	1	—	0.16	0.14	7:1
Dikes	intruding host sediments	ASI-82	50	—	—	—	—	—	—	—	—
		ASI-100	50	—	—	—	—	—	—	—	—

three component system quartz-orthoclase-albite reaches its minimum temperature of 660–700°C when the components are in equal proportions (fig. 22). This point coincides with the clustering of the modal and normative analyses of the same three components on the same triangular compositional diagram (figs. 20 and 21), thus leading to the overwhelming conclusion that the analyzed granites were truly of magmatic origin. Tuttle and Bowen (1958) went on to show that sediments at 37 km (23 mi.) depth could melt to form a granitic magma at 630°C if sufficient water were present. Johannes and Holtz (1996) have subsequently shown that at the pressure and temperature conditions indicated for the contact metamorphism of the host sediments at the granite contact (2 kb and 700°C), the Bathurst Granite would have to have been intruded with a water content of 4–5 wt% in the magma, which has been found to be a common water content for granitic magmas (Hall 1996; Johannes and Holtz 1996).

The results of both the modal and normative analyses of the granitic rocks of Bathurst Batholith in the Tarana-Sodwalls area (Tables 1 and 4A) can thus be recast or normalized so that their three components quartz, orthoclase, and plagioclase, and quartz, orthoclase, and albite respectively totalled 100% for each rock (tables 4B and 5). These compositions were then plotted on the three component triangular diagrams in Figs. 23 and 24. Not surprisingly the Bathurst Batholith granitic rock

Fig.16. The contact of the Bathurst Granite (right) with the host Lambie Group sedimentary strata in a railroad cut at grid reference 993589 in Fig. 4 (from Snelling 1974). Notice the vein-like apothyses of granite protruding into the sedimentary strata from the granite to the left of the line of contact.

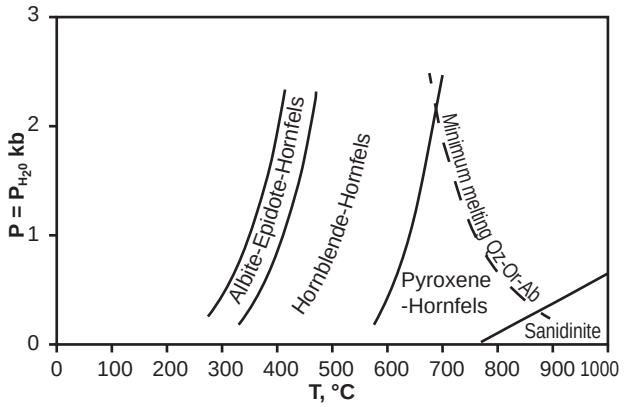

Fig. 18. Diagram showing the pressure-temperature (P-T) fields of the four facies of low-pressure contact metamorphism (after Turner 1968).

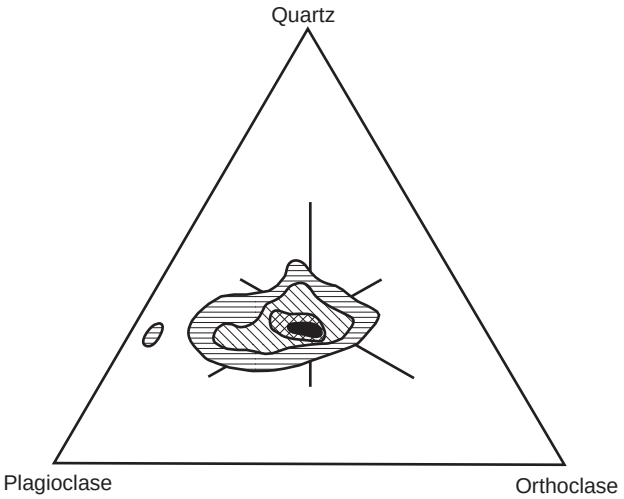

Fig. 20. Triangular plot of modal plagioclase, orthoclase and quartz in 260 thin sections of granites from the eastern United States (after Chayes 1951; Tuttle and Bowen 1958). The contours from the outside inwards are more than 0, 2, 5, and 7% respectively (0.25% counter).

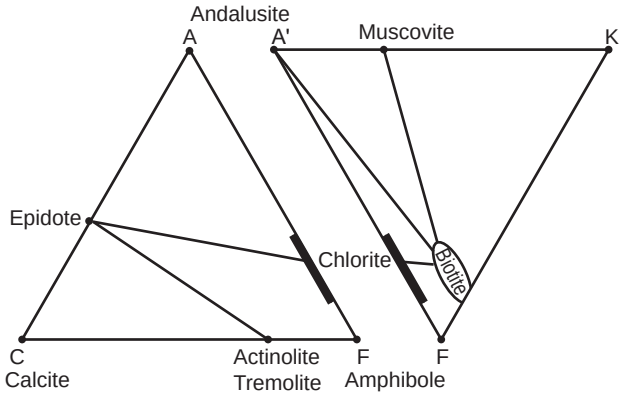

Fig.17. ACF-A′KF diagrams for the contact metamorphism of the sedimentary strata in the aureole adjoining the margin of the Bathurst Granite in the Tarana-Sodwalls area (from Snelling 1974). (A) The albite-epidote-hornfels facies. (B) The hornblende-hornfels facies.

Fig. 19. A typical granitic (acid) dike within the Bathurst Granite in a railroad cut at grid reference 963586 in Fig. 4 (from Snelling 1974). Notice the jointing in the dike and the alteration zones in the Bathurst Granite marginal to the dike due to the heat and fluids during its intrusion.

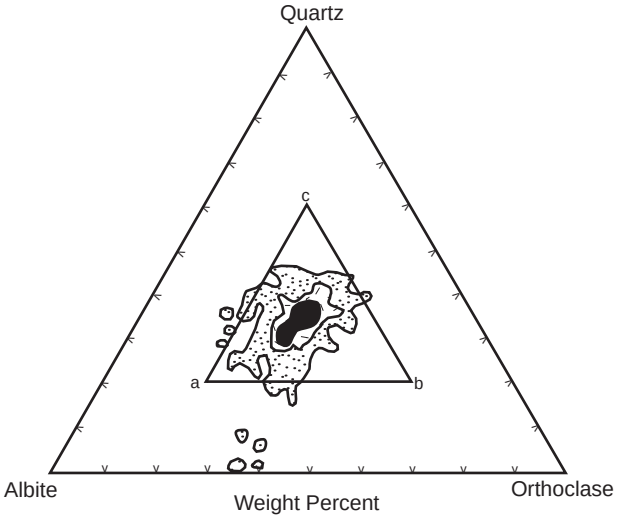

Fig. 21. Contoured triangular diagram showing the distribution of normative albite, orthoclase and quartz in all 1269 analyzed rocks in Washington's (1917) tables containing 80% or more combined albite + orthoclase + quartz (after Tuttle and Bowen 1958). The internal triangle labeled abc indicates the compositions considered to be granites (or rhyolites) in the present classification of sialic (acid) rocks.

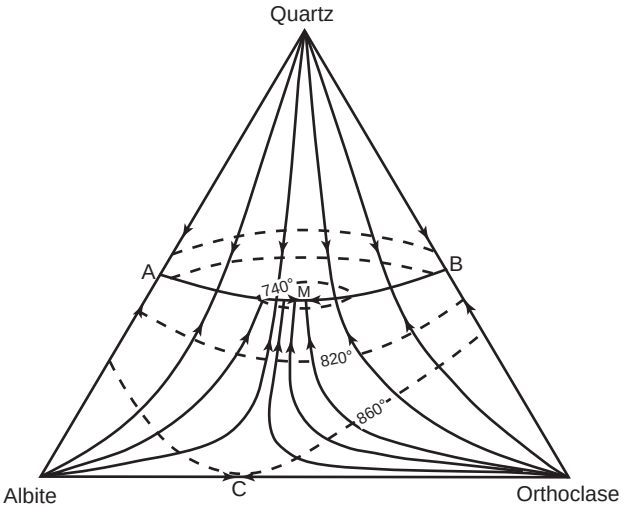

Fig. 22. Paths of crystallization in the three component (quartz+orthoclase+albite) "magma" towards the point of lowest temperature, 660–700°C (point M) (after Tuttle 1955; Tuttle and Bowen 1958).

values cluster in much the same way as Tuttle and Bowen's (1958) data (figs 20 and 21). Furthermore, a quick comparison of the modal and normative values of the Tarana-Sodwalls granitic rocks (plotted in figs. 23 and 24, respectively) with the path of magmatic crystallization to its minimum temperature of 660–700°C when the quartz-orthoclase-albite components are in equal proportions (fig. 22), demonstrates that they also coincide to Tuttle and Bowen's (1958) data (figs. 20 and 21). This suggests that the granitic rocks of the Bathurst Batholith also have a magmatic origin.

Abundant ^{238}U and ^{210}Po radiohalos are present in biotite flakes of all samples of the Bathurst Granite and Evans Crown dike (table 3 and fig. 15a–l and m–n respectively). ^{214}Po and ^{218}Po radiohalos are only present in some samples of the Bathurst Granite (table 3), but in one sample (RBG-4) they are present in comparatively large numbers, especially the ^{218}Po radiohalos. A few ^{210}Po and ^{238}U radiohalos are also present in biotite flakes within some samples of the dikes that cut across the Bathurst Granite or the Evans Crown dike (table 3 and fig. 15o–p and q–r, respectively).

The ^{238}U radiohalos in Fig. 15 are "over exposed," meaning there has been so much rapid ^{238}U decay that the resultant heavy discoloration of the biotite has blurred all the inner rings (compare with fig. 5). Often only holes remain in the centers of the ^{238}U radiohalos where the tiny zircon radiocenters have been lost during the peeling apart of the biotite flakes to tape them to the microscope slides. In Fig. 15g a visible zircon radiocenter is so large it has distorted the radiohalo's shape. In Fig. 15 there are also numerous examples of incomplete radiohalos stains. These are due to the biotite sheets not peeling apart through the radiocenters of these (spherical) radiohalos during preparation of the microscope slides. These stains usually represent ^{238}U radiohalos, but sometimes ^{210}Po radiohalos. Nevertheless, only the visible complete radiohalos where the radiocenters were visible are recorded in Table 3. The ^{210}Po radiohalos are easily identified by their single outer ring about 39μm (microns) in diameter (fig. 5).

Table 4. Normative analyses of orthoclase, albite (plagioclase) and quartz in the Bathurst Granite and Evans Crown dike of the Tarana-Sodwalls area derived from the chemical analyses in Table 1. (A) The raw normative proportions. (B) The adjusted proportions, normalized to 100%.

A.

	1	2	3	4	5	6	7	8
Orthoclase	28.36%	25.58%	29.4%	31.14%	31.69%	31.69%	28.36%	27.80%
Albite	27.25%	40.25%	28.30%	31.44%	33.01%	29.34%	17.82%	34.06%
Quartz	22.56%	21.60%	31.50%	30.06%	28.75%	33.06%	45.30%	35.52%
TOTAL	73.17%	87.53%	89.27%	92.64%	93.34%	95.09%	91.48%	97.38%

B.

	1	2	3	4	5	6	7	8
Orthoclase	36.82%	29.22%	33.01%	33.62%	33.94%	33.33%	31.00%	28.54%
Albite	34.81%	46.10%	31.71%	33.94%	35.36%	30.86%	19.48%	34.97%
Quartz	28.37%	24.68%	35.28%	32.44%	30.90%	35.81%	49.52%	36.49%
TOTAL	100.00%	100.00%	100.00%	100.00%	100.00%	100.00%	100.00%	100.00%

1. Bathurst Granite, Sodwalls. (Mackay 1959)
2. Bathurst Granite, Sodwalls. (Mackay 1959)
3. Bathurst Granite, Sodwalls. Analyst—W. G. Stone (Joplin 1963)
4. Bathurst Granite, Sodwalls. Analyst—Associated Laboratories of Australia
5. Evans Crown dike. (Mackay 1959)
6. Evans Crown dike. (Mackay 1959)
7. Evans Crown dike. Analyst—Associated Laboratories of Australia
8. Evans Crown dike. Analyst—Associated Laboratories of Australia

Table 5. Modal analyses of the Bathurst Granite and Evans Crown dike of the Tarana-Sodwalls area adjusted to only their quartz, orthoclase and plagioclase contents.

	1	2	3	4	5	6	7	8
Quartz	31.2%	31.0%	30.9%	29.7%	26.9%	27.1%	27.6%	28.5%
Orthoclase	24.0%	24.0%	33.7%	34.2%	28.3%	31.8%	33.0%	34.4%
Plagioclase	44.8%	45.0%	35..4%	36.1%	44.8%	41.1%	39.4%	37.1%

1. Bathurst Granite, Sodwalls. (Mackay 1959)
2. Bathurst Granite, Sodwalls. (Mackay 1959)
3. Bathurst Granite, Sodwalls.
4. Bathurst Granite, Sodwalls.
5. Evans Crown dike. (Mackay 1959)
6. Evans Crown dike. (Mackay 1959)
7. Evans Crown dike
8. Evans Crown dike

Usually their radiocenters are hollow "bubbles" or empty holes where former "bubbles" were destroyed, which is consistent with hydrothermal fluids having deposited the ^{210}Po atoms there, which then α-decayed to discolor the biotite and form the radiohalos. Sometimes the ^{210}Po radiocenters are only about 100 µm from the nearby ^{238}U radiocenters in the same biotite flake (fig. 15c, d, l, and m). The hydrothermal fluids thus did not have far to transport ^{222}Rn and Po from the ^{238}U radiocenters to form and supply the ^{210}Po radiocenters. This likely occurred within weeks so that the ^{238}U and ^{210}Po radiohalos formed concurrently. Fig. 15 (a, e, l, m, n, and r) shows "over-exposed" ^{210}Po radiohalos. This is indicative of a lot of ^{210}Po atoms having been in the radiocenters that then decayed. Spreading of the radiation damage is often due to the large sizes of many radiocenters, which appear to now be empty "holes" that may originally have been fluid-filled "bubbles." There are also remnants of much larger fluid inclusions in several biotite flakes (fig. 15b, e, f, h. i, q, and r). And finally, in Fig. 15e, k, o, and q are ^{210}Po radiohalos consisting of ^{210}Po radiation staining around elongated radiocenters that appear to have been fluid inclusions.

The data for all the samples from each rock unit are listed in Table 3 and summarized in Table 6. All granitic rock units contain more ^{210}Po radiohalos than ^{238}U radiohalos (except the dikes which intrude the sedimentary rocks and contain no radiohalos at all). There is a distinct pattern in the radiohalo abundances according to the sequence of intrusion of the different granitic rocks.

The radiohalo abundance for the Bathurst Granite are highly inflated by one sample, RBG-4, which comes from just on the edge of the main study area near Tarana (fig. 6). This sample comes from near a small prospector's mine where there was copper and gold mineralization found in hydrothermal veins (Raymond et al. 1998; Snelling 1974). Snelling (2005a) found that there were higher numbers of radiohalos in granites associated with hydrothermal ore veins and lodes, such as those hosted by the Land's End Granite in Cornwall, UK, and in and around the Mole Granite in the New England area of eastern Australia. Thus this solitary anomalous Bathurst Granite sample with high numbers of radiohalos (2270 ^{210}Po radiohalos, 23 ^{214}Po radiohalos, 520 ^{218}Po radiohalos, 1694 ^{238}U radiohalos, and 31 ^{232}Th radiohalos—see RBG-4 in table 3) would appear to be consistent with its proximity to an area of higher hydrothermal fluid flows, which lends support to the hydrothermal fluid flow model for Po transport to form Po radiohalos (Snelling 2000, 2005a; Snelling and Armitage 2003).

Excluding sample RBG-4, the Bathurst Granite has on average 2.22 ^{210}Po radiohalos and 2.7 total radiohalos per microscope slide, with a ratio of 1.6 ^{210}Po radiohalos for every ^{238}U radiohalo (table 6). As expected, the Meadow Flat stock, which is an

Table 6. Summary of the radiohalos data for the different granitic rock units of the Tarana-Sodwalls area, including several regional samples of the Bathurst Granite (see table 3).

Rock Unit	No. of Samples	No. of Slides	Radiohalos				No. of Radiohalos per Slide		Radio ^{210}Po:^{238}U
			^{210}Po	^{214}Po	^{218}Po	^{238}U	Total	^{210}Po	
Bathurst Granite	8 (7)	402 (351)	3043 (773)	23 (—)	527 (7)	1862 (168)	13.57 (2.70)	8.94 (2.22)	1.6:1 (4.6:1)
Meadow Flat Granite	4	200	395	1	—	131	2.64	1.98	3:1
Evans Crown dike	8 (7)	400 (350)	227 (226)	—	—	34 (34)	0.65 (0.74)	0.57 (0.65)	6.7:1 (6.6:1)
Dikes through Bathurst Granite	4	200	5	—	—	—	0.03	0.03	—
Dikes through Evans Crown dike	2	100	7	—	—	1	0.08	0.07	7:1
Dikes through the host sedimentary rocks	2	100	—	—	—	—	—	—	—

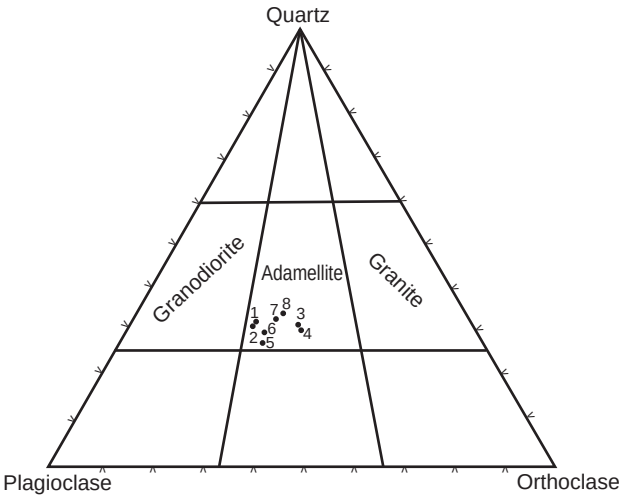

Fig. 23. Triangular plot of the modal quartz, orthoclase and plagioclase in the samples of the Bathurst Granite and the Evans Crown dike in the Tarana-Sodwalls area as recorded and numbered in Table 4. All samples plot within the adamellite field.

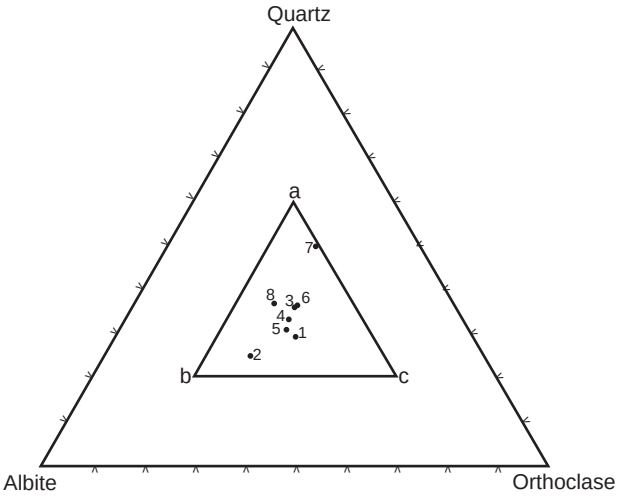

Fig. 24. Triangular plot of the normative quartz, orthoclase and albite in the samples of the Bathurst Granite and the Evans Crown dike in the Tarana-Sodwalls area as recorded and numbered in Table 5. All samples plot within the triangle abc indicating the compositions are granites as formally classified..

outlying extension of the Bathurst Granite, has similar radiohalo statistics to the Bathurst Granite, with an average of 1.98 ^{210}Po radiohalos and 2.64 total radiohalos per microscope slide, with a ratio of 3 ^{210}Po radiohalos for every ^{238}U radiohalo. In contrast, the coarse-grained inner section of the Evans Crown dike has on average 0.65 ^{210}Po radiohalos and 0.74 total radiohalos per microscope slide, but a ratio of 6.6 ^{210}Po radiohalos for every ^{238}U radiohalo (see the samples in brackets in table 6, compared to the total figures that include the sample from the fine-grained margin). Similarly, radiohalo numbers are low in the dikes cutting through the Bathurst Granite and Evans Crown dike, with averages of 0.03 ^{210}Po radiohalos and 0.03 total radiohalos per microscope slide and 0.07 ^{210}Po radiohalos and 0.08 total radiohalos per microscope slide, respectively. But the ratio at seven ^{210}Po radiohalos for every ^{238}U radiohalo in the dikes cutting through the Evans Crown dike is higher.

Results compared to previous models

In conventional thought, the Po radiohalos observed in the Bathurst Granite are "a very tiny mystery" (G. Brent Dalrymple, as quoted by Gentry, 1988, p. 122) that can be conveniently ignored because they have little apparent significance. However, the reality is that the mystery of the Po radiohalos is often ignored because it constitutes a profound challenge to conventional wisdom.

Comprehensive reviews of what these Po radiohalos are and how they may have formed are provided by Gentry (1973, 1974, 1986, 1988) and Snelling (2000). Gentry (1974) has established that all the observed Po radiohalos are generated exclusively from the Po radioisotopes in the ^{238}U decay series, namely, ^{218}Po, ^{214}Po, and ^{210}Po, with contributions from none of the other species in the ^{238}U α-decay chain. Furthermore, it has been estimated that, like the ^{238}U radiohalos, each visible Po radiohalo requires between 500 million and 1 billion α-decays (Gentry 1988), equating to a corresponding number of Po atoms in each radiocenter. Yet the half-lives of these Po radioisotopes are only 3.1 minutes (^{218}Po), 164 microseconds (^{214}Po), and 138 days (^{210}Po), so how did so many Po atoms get concentrated into these radiocenters, before they decayed, to then generate the Po radiohalos?

Gentry (1986, 1988, 1989) insists that the Po must be primordial, that is, God created the Po radioisotopes instantaneously in place in the radiocenters in the biotite flakes in the granites, and thus the granites are also created rocks. In other words, he argues that granites did not form from the crystallization and cooling of magmas, but rather are the earth's original foundation rocks.

Moreover, where granites such as the Bathurst Granite have intruded into fossiliferous Flood-deposited strata, Gentry (1989) insists that these granites also represent originally created rocks. He argues that during the Flood they were tectonically intruded as cold bodies, and that the contact metamorphic aureoles were produced by the heat and pressure generated during tectonic emplacement, augmented in some cases by hot fluids from depth. Thus, in the case of the Bathurst Granite, he would surmise it was tectonically emplaced during the Flood, but he would have to also argue that the Evans Crown dike and the dikes intruding it and the Bathurst Granite were subsequently and

sequentially emplaced tectonically. Alternately he would argue the Bathurst Granite was created then tectonically emplaced during the Flood, yet somehow the Evans Crown and the other dikes were then sequentially intruded into the Bathurst Granite and the host sediments.

Such interpretations are inconsistent with the field and petrological evidence from the Bathurst Granite and the dikes, and with the experimental evidence discussed above. The contact between the Bathurst Granite and the regionally metamorphosed fossiliferous (Flood-deposited) host rocks it intruded is a sharp, knife-edge boundary, with none of the fracturing, brecciation, or mylonization that should be evident in either the granite or host rocks if the granite had been intruded tectonically as a cold body (fig. 16). Instead, there are apothyses or veins of granite intruding into the host sedimentary layers, and a contact metamorphic aureole with mineralogy consistent with the temperatures of the granite magma when it intruded (figs. 18 and 22). Furthermore, the mineralogy and textures of the Evans Crown dike and the dikes which intrude into it and the Bathurst Granite are very similar to and identical with those of the Bathurst Granite (fig. 14). This is entirely consistent with a magmatic origin for all these granitic phases from the same magma source, but is not in any way consistent with the Bathurst Granite being created cold and the subsequent granitic dikes being a result of local melting of the Bathurst Granite during its cold tectonic emplacement during the Flood. The chilled margin of the Evans Crown dike against the Bathurst Granite and the host sedimentary rocks is also consistent with its intrusive magmatic origin.

Gentry (1989) postulated hot fluids augmented the heat and pressure during tectonic emplacement of cold granite bodies to produce the contact aureoles, and presumably the local melting of the granite at its margin to produce veins and apothyses, and in the case of the Bathurst Granite, also the formation of the granitic magma that then intruded as the Evans Crown dike and subsequent dikes. However, if the theorized accompanying hot fluids from depth had a temperature of >150°C, as likely they would have to locally melt granite, then they would have left evidence of their passage within the Bathurst Granite and annealed all the radiohalos in it (Laney and Laughlin 1981). There is no observable evidence of any pervasive alteration produced by hydrothermal fluids, either macroscopically or microscopically, in the Bathurst Granite. In fact, the only evidence of extensive hydrothermal fluid flows in the Bathurst Granite is in the one sample (RBG-4) in proximity to hydrothermal ore veins, showing an increase in the numbers of Po radiohalos, consistent with the hydrothermal fluid model for transport of the Po atoms as a requirement to form the Po radiohalos (Snelling 2005a; Snelling and Armitage 2003).

Evidence supporting the hydrothermal fluid transport model

We conclude that the presently observed Po radiohalos in the Bathurst Granite and its associated granitic dikes could only have been generated after the granite had cooled below 150°C (Laney and Laughlin 1981). Thus the Po radiohalos were formed after the Bathurst Granite was intruded as magma and after it and its contact metamorphic aureole in the host rocks had cooled. The only other model at present that explains the formation of the Po radiohalos is the hydrothermal fluid transport model (Snelling 2005a; Snelling and Armitage 2003). In that model it is postulated that the Po isotopes, as well as the ^{222}Rn parent of ^{218}Po, were produced from ^{238}U decay in the zircons which are the radiocenters of nearby ^{238}U radiohalos located in the same biotite flakes as the Po radiohalos. The hydrothermal fluids released by the crystallizing and cooling granite magma flowed along the biotite cleavage planes and transported the ^{222}Rn and Po isotopes from the zircon radiocenters (fig. 25). The Po isotopes, including the ^{218}Po produced by ^{222}Rn α-decay (half-life of 3.8 days), likely precipitated in lattice defects along the same biotite cleavage planes where S, Cl, and other atoms chemically attractive to Po were located, remaining within about a millimeter of the zircon radiocenters. These Po precipitation sites became the subsequent radiocenters for the Po radiohalos. As the Po in the radiocenters α-decayed, new Po atoms were supplied from hydrothermal fluids flowing through the biotite lattice (fig. 25). Thus, provided the supply of Po isotopes was sufficient and the hydrothermal fluid flows were sustained and rapid, the required Po concentrations could have been supplied to the radiocenters to produce the 500 million–1 billion Po α-decays to generate the Po radiohalos within hours or days, consistent with the very short half-lives of the Po isotopes.

Because hydrothermal fluid flows are crucial to this Po radiohalos formation model, it might be expected that the greater the volume and flow of hydrothermal fluids, the greater the probability that more Po radiohalos would be generated. This prediction has shown to hold true in several situations. First, in granites where hydrothermal ore deposits have formed in veins due to large, sustained hydrothermal fluid flows, there are huge numbers of Po radiohalos (for example, the Land's End Granite, Cornwall [Snelling 2005a]). Second, where hydrothermal fluids were produced by mineral reactions, at a specific pressure-temperature boundary during regional

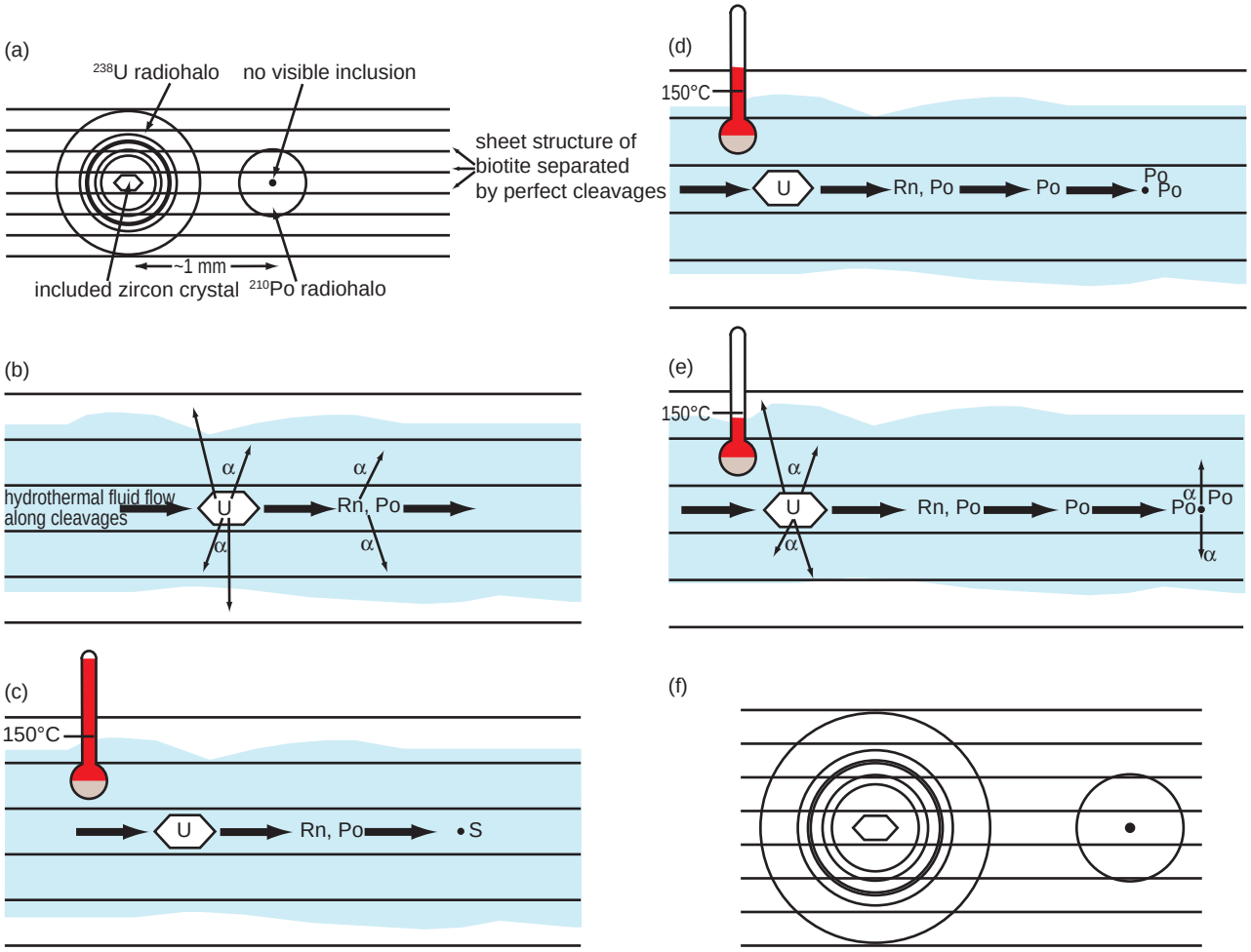

Fig. 25. Time sequence of diagrams to show schematically the formation of ^{238}U and ^{210}Po radiohalos concurrently as a result of hydrothermal fluid flow along the biotite flakes within a cooling granite mass (after Snelling 2005a).
(a) Diagrammatic cross-section through a biotite flake showing the sheet structure and perfect cleavage. A tiny zircon crystal (left) has been included between two sheets and its ^{238}U content has generated a ^{238}U radiohalo. A ^{210}Po radiohalo (right) has also developed around a tiny radiocenter between the same two sheets. Its radiocenter contains no visible inclusion, being just a bubble-like "hole" left behind by loss of the original inclusion, probably by dissolution of the solid phases.
(b) Enlarged diagrammatic cross-section through a biotite flake that has crystallized from a granite magma to 300°C. The radioactive ^{238}U in an included zircon crystal is emitting α-particles, while hydrothermal fluids released from the cooling magma are flowing along the cleavage planes dissolving the U decay products—^{222}Rn and Po isotopes—that have diffused out of the tiny zircon crystal and carrying them downflow a short distance where they also emit α-particles.
(c) However, at temperatures >150°C the α-tracks are annealed, so no radiohalos form and there is no α-track record of the hydrothermal fluids containing Rn and Po flowing at a rate of up to 5 cm (2 in) per day along the cleavage plane. A few S atoms also transported in the hydrothermal fluids become lodged in lattice defects downflow of the zircon crystal.
(d) As the temperatures approach 150°C and ^{222}Rn decays to ^{218}Po, the Po isotopes in the hydrothermal fluids which have a geochemical affinity for S precipitate to form PoS as the fluids flow by the S atoms in the lattice defects. The ^{238}U in the zircon continues to decay and replenish the supply of Rn and Po isotopes in the fluids.
(e) Once the temperature drops to below 150°C, the α-tracks produced by continued decay of both the ^{238}U in the zircon and the Po in the PoS are no longer annealed and so start discoloring the biotite sheets, forming both ^{238}U and ^{210}Po radiohalos concurrently. More Po isotopes in the flowing hydrothermal fluids replace the Po in the PoS after it decays to Pb, the "freed" S atoms scavenging yet more Po from the passing fluids.
(f) With further passing of time and more α-decays both the ^{238}U and ^{210}Po radiohalos are fully formed, the granite cools completely and hydrothermal fluid flow ceases. Note that both radiohalos have to form concurrently below 150°C, and that the original content at the center of the ^{210}Po radiohalo has been dissolved and carried away. The rate at which these processes occur must therefore be governed by the 138 day half-life of ^{210}Po. To get ^{218}Po and ^{214}Po radiohalos the processes would have to have occurred even faster.

metamorphism, four to five times more Po radiohalos were generated, precisely at that specific metamorphic boundary (Snelling 2008b). Third, the Po radiohalos numbers also progressively decreased where the hydrothermal fluids generated in the central granite at the highest grade within a regional metamorphic complex flowed and decreased outwards into that complex (Snelling 2008c). Fourth, in a granite pluton which has an atypically wide contact metamorphic and metasomatic aureole around it due to the high volume of hydrothermal fluids it released during its crystallization, Po radiohalos numbers were shown to be higher than in other granite plutons (Snelling 2008d). Fifth, in a sequentially intruded suite of nested granite plutons where the hydrothermal fluid content of the granites correspondingly increased, so that the last intruded central pluton was connected to coeval explosive, steam-driven volcanism, the numbers of Po radiohalos generated increased inwards within the nested suite of granite plutons (Snelling and Gates 2009). Such evidence provides confirmation that the hydrothermal fluid transport model can explain the generation of the Po radiohalos.

Suggested model for the Bathurst Granite

The hydrothermal fluids generated by the crystallization and cooling of the Bathurst Granite produced several effects indicating a large volume of sustained fluid flow was involved. Hydrothermal fluids dispersed the heat released by the crystallizing granite by convection into the host rocks. The heat from these fluids likely helped to generate the contact metamorphic aureole around the granite (Mackay 1959; Snelling 1974). Additionally, in one location near Tarana, the hydrothermal fluids penetrated along fractures in the host rocks, beyond the aureole, to deposit ore veins of copper and gold (Raymond et al. 1998; Snelling 1974). Then, within the granite itself, the numbers of Po radiohalos are consistent with sustained hydrothermal fluid flows. The tiny zircon grains that are still at the centers of the many ^{238}U radiohalos in the Bathurst Granite would have been the source of the Po isotopes transported by the hydrothermal fluids to generate the Po radiohalos. However, the general absence of ^{214}Po and ^{218}Po radiohalos in the Bathurst Granite and the granitic dikes implies both a generally reduced supply of hydrothermal fluids and a slow rate of hydrothermal fluid transport, restricting the formation of those radiohalos due to their very short half-lives. It also implies that ^{222}Rn was likely absent in the hydrothermal fluids. Therefore, Po was most likely transported primarily as ^{210}Po in the fluids to the nucleation sites where the ^{210}Po radiohalos formed.

A constraining factor on the preservation of the Po radiohalos is that the damage left by the α-particles is retained in the biotite flakes only below 150°C (Laney and Laughlin 1981). Above this α-particle annealing temperature the damage either doesn't register or is obliterated. Thus all the radiohalos now observed in the Bathurst Granite had to form below 150°C, late in the cooling history of the granite. Granite magmas intrude at temperatures of 650–750°C, and the hydrothermal fluids are released at temperatures of 370–410°C, after most of the constituent minerals have crystallized (fig. 26). However, the accessory zircon grains, containing the ^{238}U, crystallize very early at higher temperatures, and likely were already formed in the magma before and during intrusion. Thus the ^{238}U decay producing the Po isotopes had begun well before the granite had fully crystallized, and before the hydrothermal fluids had begun flowing. Furthermore, by the time the temperature of the granite and the hydrothermal fluids had cooled to 150°C, the heat energy driving hydrothermal fluid convection would have likely begun to wane and the vigor of the hydrothermal flow would also have begun to diminish (fig. 26). If the processes of magma intrusion, crystallization and cooling required 100,000–1 million years, as is conventionally claimed (Pitcher 1993; Young and Stearley 2008), most of the Po would have already decayed and thus been lost from the hydrothermal fluids by the time the granite and fluids had cooled to 150°C, leaving no Po isotopes left to generate the Po radiohalos (Snelling 2008a).

The data in Tables 3 and 6 show that Po radiohalos greatly outnumber ^{238}U radiohalos in the Bathurst Granite. There are likely two reasons for this. First, many of the ^{238}U radiohalos are dark and overexposed with blurred inner rings (fig. 15), which indicates that there has been an enormous amount of ^{238}U decay, much more than the 500 million–1 billion atoms needed to produce a radiohalo with distinct inner rings. This implies that there likely would have been enough Po generated to form multiple Po radiohalos in the vicinity of each ^{238}U radiohalo. Second, as noted above, much evidence suggests that the greater the volume and flow of hydrothermal fluids, the greater the number of Po radiohalos generated. A reasonably large volume of hydrothermal fluids apparently flowed within and through the Bathurst Granite and the associated dikes. Thus, there was a great capacity for hydrothermal fluid transport of Po atoms to supply the observed Po radiohalos.

Rapid formation of the Bathurst Granite

Conventional thinking on the timescale for the granite intrusion, crystallization, and cooling processes used to claim granite formation took more than a million years (Pitcher 1993; Young and Stearley 2008). However, it is now recognized

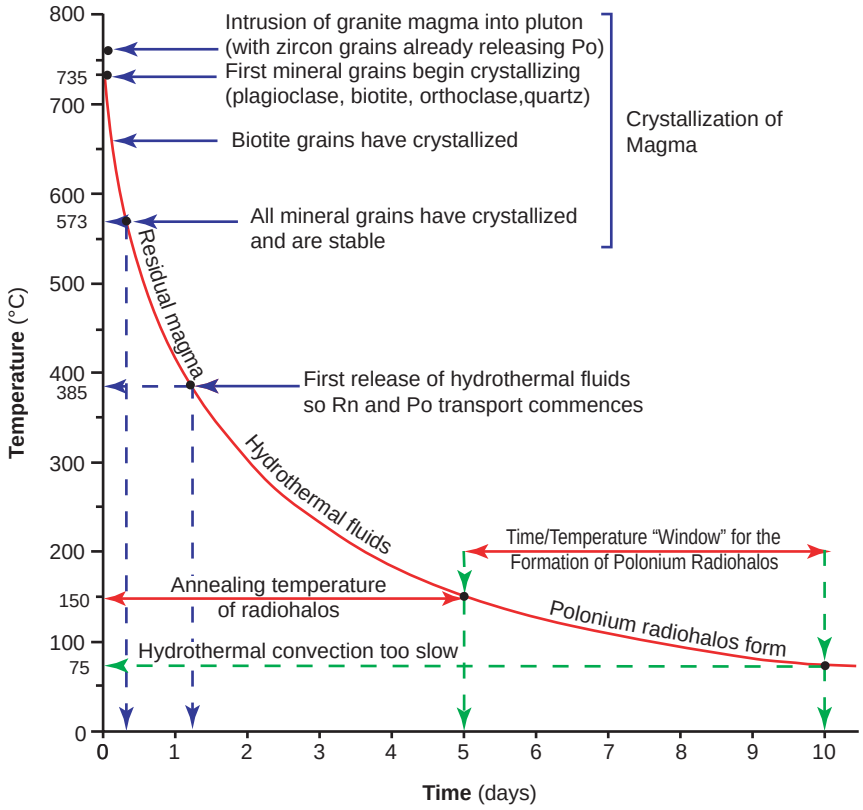

Fig. 26. Schematic, conceptual, temperature versus time cooling curve diagram to show the timescale for granite crystallization and cooling, hydrothermal fluid transport, and the formation of polonium radiohalos (after Snelling 2008a).

that granite formation is a rapid, dynamic process operating on timescales as short as thousands of years (Clemens 2005; Petford et al. 2000). Various studies have shown that emplacement of a melt is rapid via dikes and fractures, and assisted by tectonics (Clemens and Mawer 1992; Coleman, Gray, and Glazner 2004). Other studies have shown that melt cooling is aided by hydrothermal fluids and groundwater flow (Brown 1987; Burnham 1997; Cathles 1977; Hardee 1982; Hayba and Ingebritsen 1997). Formation of these granites, from emplacement to cooling, therefore had to have been on a timescale that previously has been considered impossible. The processes of magma generation, segregation, ascent, emplacement, crystallization, and cooling are now being viewed even as catastrophic (Snelling 2008a, Snelling and Woodmorappe 1998; Vardiman, Snelling, and Chaffin 2005).

Catastrophic granite formation and accelerated decay

Both catastrophic granite formation and accelerated radioisotope decay are relevant to the hydrothermal fluid transport model for Po radiohalo formation (Vardiman, Snelling, and Chaffin 2005). Halo formation provides constraints on the rates of both those processes (Snelling 2005a). If ^{238}U in the zircon radiocenters supplied the Po isotopes required to generate the Po radiohalos, the ^{238}U and Po radiohalos must have formed in hours or days, as required by the Po isotopes' short half-lives. This requires ^{238}U production of Po to be grossly accelerated. The 500 million–1 billion α-decays necessary to generate each ^{238}U radiohalo, equivalent to at least 100 million years' worth of ^{238}U decay at today's decay rates, had to have taken place in hours to days to supply the required concentration of Po for producing Po radiohalos. However, because accelerated ^{238}U decay in the zircons would have occurred as the zircons crystallized at 650–750°C (fig. 26), the granite magma must have fully crystallized and cooled to below 150°C very rapidly. If not, the ^{238}U in the zircons would have rapidly decayed away, as would have also the daughter Po isotopes, before the biotite flakes were cool enough for the ^{238}U and Po radiohalos to form and survive without annealing. Furthermore, the hydrothermal fluid flows needed to transport the Po isotopes along the biotite cleavage planes from the zircons to the Po radiocenters are not long sustained, even in the conventional framework, but decrease rapidly due to cooling of the granite (fig. 26) (Snelling 2008a).

Therefore, Snelling (2005a) concluded that granite intrusion, crystallization, and cooling processes occurred together over a timescale of only about 6–10 days.

Thus sufficient Po had to be transported quickly to the Po radiocenters to form the Po radiohalos while there was still enough energy at and below 150°C to drive the hydrothermal fluid flows rapidly enough to get the Po isotopes to the deposition sites before they decayed. This is the time and temperature "window" depicted schematically in Fig. 26. It would thus simply be impossible for the Po radiohalos to form slowly over many thousands of years at today's groundwater temperatures and chemistries in cold granites. Hot chemically enriched hydrothermal fluids are needed to dissolve and carry the Po atoms, and heat is needed to drive rapid hydrothermal convection to move Po transporting fluids fast enough to supply the Po radiocenters to generate the Po radiohalos. Furthermore, the required heat cannot be sustained for the 100 million years or more while sufficient ^{238}U decays at today's rates to produce the 500 million–1 billion Po atoms needed for each Po radiohalo.

One consequence of accelerated ^{238}U decay is that the decay of the Po isotopes might also be similarly accelerated, and thus there would not have been enough time for hydrothermal fluid transport of the radioactive Po atoms within the biotite flakes. However, Austin (2005) and Snelling (2005b) have shown that in an accelerated α-decay episode the parent isotopes which today have the slowest decay rates (and thus yield the oldest ages on the same rock samples) had their decay accelerated the most. The implication of this observation is that in an accelerated α-decay episode, the Po isotopes which decay at extremely high rates today should have experienced almost no acceleration of their decay. This inverse relationship of decay rate to accelerated decay would, therefore, have allowed enough time for hydrothermal fluid transport of the Po atoms to generate the Po radiohalos.

However, what requires the hydrothermal fluid flow interval to be so brief? Surely, because the zircon radiocenters and their ^{238}U radiohalos are near to (typically within only 1 mm [0.04 in] or so) the Po radiocenters in the same biotite flakes, could not the hydrothermal flow have indeed carried each Po atom from the ^{238}U radiocenters to the Po radiocenters within minutes, but the interval of hydrothermal fluid flow persist over many thousands of years during which the billion Po atoms needed for each Po radiohalo are transported that short distance? In this case the ^{238}U decay and the generation of Po atoms could be stretched over that longer interval. However, as already noted above, by the time a granite body and its hydrothermal fluids cool to below 150°C, most of the energy to drive the hydrothermal convection system and fluid flow has already dissipated (Snelling 2008a). The hydrothermal fluids are expelled from the crystallizing granite and start flowing at between 410 and 370°C (fig. 26), so unless the granite cooled rapidly from 400°C to below 150°C, most of the Po transported by the hydrothermal fluids would have been flushed out of the granite by the vigorous hydrothermal convective flows as they diminished. Simultaneously, much of the energy to drive these fluid flows dissipates rapidly as the granite temperature drops. Thus, below 150°C (when the Po radiohalos start forming) the hydrothermal fluids have slowed down to such an extent that they cannot sustain protracted flow. Moreover, the capacity of the hydrothermal fluids to carry dissolved Po decreases dramatically as their temperature decreases.

In summary, for there to be sufficient Po to produce Po radiohalos after the Bathurst Granite cooled to 150°C, the timescales of the decay process as well as the cooling both must be on same order as the lifetimes of the Po isotopes. The hydrothermal fluid flows had to be rapid, as the convection system was short-lived while the granite crystallized and cooled rapidly within 6–10 days, and as they transported sufficient Po atoms to generate the Po radiohalos within hours to a few days.

Furthermore, if the formation of the large volume, Bathurst Granite was rapid in order for the radiohalos present in it to exist, it follows that the formation of the intruded granitic dikes in this field area which also contain Po radiohalos had to be likewise rapid. The numbers of Po radiohalos in these subsequent granitic dikes decrease in order of their intrusion, with the narrower granitic dikes containing fewer Po radiohalos intruded after the Evans Crown dike (table 6). On the other hand, the ratio of ^{210}Po radiohalo numbers per each ^{238}U radiohalo increases according to the time sequence in which these units were intruded, from around 4:1 in the Bathurst Granite to 6.6:1 in the Evans Crown dike to 7:1 in the granitic dikes intruding the Evans Crown dike. This is consistent with an increase in hydrothermal fluids being progressively released with each subsequent granitic intrusion. This is further corroborated by the evidence of increased hydrothermal alteration observed in the Evans Crown dike and the subsequently intruded granitic dikes (fig. 14), and is consistent with all these granitic rocks being sourced from the same magma body late in its "life." Thus the granitic magma that was intruded as the Evans Crown dike was likely residual magma from the Bathurst Granite, while the remaining residual magma then intruded into the Evans Crown dike. Such an increase in the volume of hydrothermal

fluids in a sequence of granitic intrusions has already been documented by Snelling and Armitage (2003) in the zoned La Posta Pluton in the Peninsular Ranges Batholith east of San Diego, and by Snelling and Gates (2009) in the nested plutons of the Tuolumne Intrusive Suite of Yosemite, California.

Thus the significance of the progressively increasing Po radiohalo numbers relative to ^{238}U radiohalos numbers in granitic intrusions within the Bathurst Batholith (table 6), according to the order in which they were intruded, implies that there were progressively more hydrothermal fluids per volume with each successive intrusion from the Bathurst Granite pluton to the large Evans Crown dike to the narrow granitic dikes intruding them both. The increase in the hydrothermal fluids in the later stages of the intrusive sequence is likely due to the water released as the intrusive phases crystallized and cooled building up in the later residual intrusive phases; particularly if the hydrothermal fluids are not readily escaping out into the surrounding host rocks. Whereas many other granite plutons intruded into sedimentary rocks containing connate and ground waters that assisted rapid granite cooling by convection outwards from the plutons (Snelling and Woodmorappe 1998), the large Evans Crown dike intruded into the Bathurst Granite pluton, and then narrower granitic dikes subsequently intruded into them both. Consequently, since granites have poor connective porosities and therefore poor permeabilities, the successively generated hydrothermal fluids would have been essentially "trapped" in the later intrusive phases.

Since these granitic intrusions in the Bathurst Batholith were successively intruded into one another, there were severe constraints, due to the 150°C thermal annealing temperature of the radiohalos. The lapse of time between the intrusion of each phase of the batholith had to be extremely short, as each phase had to be rapidly emplaced, crystallized and cooled before the next phases were injected, so that the entire intrusion sequence of pluton and dikes was in place before the radiohalos began forming below 150°C. Otherwise, the heat given off by each successively emplaced phase, which intruded its predecessors, would have annealed all radiohalos in them. Confirmation that each phase had crystallized and cooled before the next phase was intruded is demonstrated by the lack of contact metamorphic effects where the Evans Crown dike intrudes the Bathurst Granite and where the smaller dikes cut into the Bathurst Granite and the Evans Crown dike, by the chilled margin of the Evans Crown dike, and by alteration zones marginal to the smaller dikes (Snelling 1974). It can therefore be concluded that the successive development of the batholith was a relatively rapid emplacement process. However, so that annealing of the radiohalos would not occur above 150°C, all the phases of the batholith had to have intruded so rapidly that the Bathurst Granite pluton, and the stocks, satellite bodies, and subsequent large and small dikes making up the batholith cooled below 150°C more or less at the same time. Furthermore, because of the short half-life of ^{210}Po and the need for the hydrothermal fluids within the cooling granite masses to rapidly transport sufficient ^{210}Po to supply the radiocenters to form the ^{210}Po radiohalos before the ^{210}Po decayed, the successive emplacement and cooling of this successive series of intrusions could not have taken more than a week or two.

Survival of the Po radiohalos as a result of the rapid sequential emplacement of these intrusions also implies that there could not have been a "heat problem" due to accelerated radioactive decay (Snelling 2005a). The mechanisms that dissipated the heat from these crystallizing and cooling magmas (Snelling 2008a; Snelling and Woodmorappe 1998) did so rapidly and efficiently without annealing the Po radiohalos in the surrounding earlier intruded phases of this suite of intrusions. Thus this entire intrusive event that lasted only a week or two, consisting of successive pulses of granite magma emplacement and cooling, fits easily within the time frame of the year-long Flood event.

Extension of model to other granites

The Bathurst Granite does not appear to be unique, but rather is typical of other granites, in terms of its mineralogy, chemistry, texture, and the hydrothermal fluids it generated. Thus this model for its rapid formation and cooling can be extended to other granite bodies, as has been done by Snelling (2005a, 2008a, d), Snelling and Armitage (2003), and Snelling and Gates (2009). Many other granites are surrounded by aureoles, though many are often larger. Almost all granites show evidence of the hydrothermal fluids they generated as they crystallized and cooled. The ubiquitous presence of Po radiohalos (Snelling 2005a) is also testimony to these hydrothermal fluids. In those granites where fewer Po radiohalos suggest less hydrothermal fluids were produced, the presence of Po radiohalos indicates there were still sufficient hydrothermal fluids to cool them rapidly. The volume of the Bathurst Batholith is very large. Yet, the volume of the nested granite plutons of the Tuolumne Intrusive Suite of Yosemite, California, is comparable to that of the Bathurst Batholith, and Snelling and Gates (2009) built a strong case that each of those plutons also formed and cooled rapidly. Because this model of rapid formation and cooling has been applied successfully to other

granite bodies, it can be concluded that each of the plutons, stocks, satellite bodies and subsequent large and small dikes making up the Bathurst Batholith likewise formed and cooled rapidly.

Conclusions

The Bathurst Granite intruded Flood-deposited, fossiliferous sedimentary strata, disrupting them and producing a contact metamorphic zone. It was then itself intruded by the Evans Crown dike, which has a chilled margin. Finally, smaller granite dikes intruded both the Bathurst Granite, Evans Crown dike and the host sedimentary strata, producing adjacent alteration zones. Field and textural data have established that these granite phases were sequentially intruded while still hot. Analytical and experimental data confirm that these granitic phases were intruded rapidly as hot magma, contradicting Gentry's concept of their cold creation and tectonic emplacement during the Flood. Evidence suggests all granitic phases were intruded from the same magma source, with the release of hydrothermal fluids as the magmas crystallized and cooled. All three granite phases contain ^{238}U and Po radiohalos. The Po radiohalos indicate rapid formation after all the granites cooled below 150°C via hydrothermal fluid transport of Po from ^{238}U decay in the zircon grains in the biotite flakes that are usually in the radiocenters of the ^{238}U radiohalos. Their presence in all three, sequentially intruded, granite phases is evidence that all this intrusive activity, and the cooling of all three granite phases to below 150°C, must have occurred within a week or two so that the Po radiohalos in them subsequently formed within days to weeks during the Flood year.

References

Austin, S.A. 2005. Do radioisotope clocks need repair? Testing the assumptions of isochron dating using K-Ar, Rb-Sr, Sm-Nd, and Pb-Pb isotopes. In *Radioisotopes and the age of the earth: Results of a young-earth creationist research initiative*, ed. L. Vardiman, A.A. Snelling and E.F. Chaffin, pp. 325–392. El Cajon, California: Institute for Creation Research, and Chino Valley, Arizona: Creation Research Society.

Benson, W.N. 1907. The geology of Newbridge, near Bathurst, N.S.W. *Proceedings of the Linnean Society of New South Wales* 32:523–553.

Binns, R.A. 1958. *The geology of the Cow Flat District, near Bathurst, N.S.W.* B.Sc. (Hons) Thesis (unpublished), The University of Sydney, Australia.

Branagan, D.F., and G.H. Packham. 2000 Field geology of New South Wales. 3rd ed. Sydney, Australia: Department of Mineral Resources.

Brown, S.R. 1987. Fluid flow through rock joints: The effect of surface roughness. *Journal of Geophysical Research* 92:1337–1347.

Bucher, K., and M. Frey. 2002. *Petrogenesis of metamorphic rocks*. Berlin, Germany: Springer-Verlag.

Burnham, C.W. 1997. Magmas and hydrothermal fluids. In *Geochemistry of hydrothermal ore deposits*. 3rd ed., ed. H.L. Barnes, pp. 63–123. New York, New York: Wiley.

Cas, R.A.F., R.H. Flood, and S.E. Shaw. 1976. Hill End Trough: New radiometric ages. *Search* 7:205–207.

Cathles, L.M. 1977. An analysis of the cooling of intrusives by ground-water convection which includes boiling. *Economic Geology* 72:804–826.

Chaffer, J.A.F. 1955. *Geology of the Tarana-Diamond Swamp Creek area*. B.Sc. (Hons) Thesis (unpublished), The University of Sydney, Australia.

Chappell, B.W., P.M. English, P.L. King, A.J.R. White, and D. Wyborn. 1991. Granites and related rocks of the Lachlan Fold Belt (1:250,000). Canberra, Australia: Bureau of Mineral Resources, Geology and Geophysics.

Chayes, F. 1951. Modal composition of granites. *Carnegie Institution of Washington Year Book* 50:41.

Clemens, J.D. 2005. Granites and granitic magmas: Strange phenomena and new perspectives on some old problems. *Proceedings of the Geologists' Association* 116:9–16.

Clemens, J.D., and C.K. Mawer. 1992. Granitic magma transport by fracture propagation. *Tectonophysics* 204: 339–360.

Coleman, D.S., W. Gray, and A.F. Glazner. 2004. Rethinking the emplacement and evolution of zoned plutons: Geochronologic evidence for incremental assembly of the Tuolumne Intrusive Suite, California. *Geology* 32, no. 5:433–436.

Facer, R.A. 1979. New and recalculated radiometric data supporting a Carboniferous age for the emplacement of the Bathurst Batholith, New South Wales. *Journal of the Geological Society of Australia* 25, no. 8:429–432.

Gentry, R.V. 1968. Fossil alpha-recoil analysis of certain variant radioactive halos. *Science* 160:1228–1230.

Gentry, R.V. 1970. Giant radioactive halos: Indicators of unknown radioactivity. *Science* 169: 670–673.

Gentry, R.V. 1971. Radiohalos: Some unique lead isotopic ratios and unknown alpha activity. *Science* 173:727–731.

Gentry, R.V. 1973. Radioactive halos. *Annual Review of Nuclear Science* 23:347–362.

Gentry, R.V. 1974. Radiohalos in a radiochronological and cosmological perspective. *Science* 184:62–66.

Gentry, R.V. 1986. Radioactive halos: Implications for creation. In *Proceedings of the First International Conference on Creationism*, ed. R.E. Walsh, C.L. Brooks, and R.S. Crowell, vol. 2, pp. 89–100. Pittsburgh, Pennsylvania: Creation Science Fellowship.

Gentry, R.V. 1988. *Creation's tiny mystery*. Knoxville, Tennessee: Earth Science Associates.

Gentry, R.V. 1989. Response to Wise. *Creation Research Society Quarterly* 25:176–180.

Hall, A. 1996. *Igneous petrology*. 2nd ed. Harlow, England: Addison Wesley Longman Limited.

Hardee, H.C. 1982. Permeable convection above magma bodies. *Tectonophysics* 84:179–195.

Hayba, D.O. and S.E. Ingebritsen. 1997. Multiphase groundwater flow near cooling plutons. *Journal of Geophysical Research* 102:12,235–12,252.

Henderson, G.H., and S. Bateson. 1934. A quantitative study of pleochroic haloes—I. *Proceedings of the Royal Society of London*, Series A 145:563–581.

Henderson, G.H., G.M. Mushkat, and D.P. Crawford. 1934. A quantitative study of pleochroic haloes—III Thorium. *Proceedings of the Royal Society of London*, Series A 158:199–211.

Holmes, A. 1931. Radioactivity and geological time. In Physics of the earth—IV. The age of the earth. *Bulletin of the National Research Council* 80:124–460.

Iimori, S., and J. Yoshimura. 1926. Pleochroic halos in biotite: Probable existence of the independent origin of the actinium series. *Scientific Papers of the Institute of Physical and Chemical Research* 5, no.66:11–24.

Johannes, W., and F. Holtz. 1996. *Petrogenesis and experimental petrology of granitic rocks*. Berlin, Germany: Springer-Verlag.

Joly, J. 1917a. Radio-active halos. *Philosophical Transactions of the Royal Society of London*, Series A 217:51–79.

Joly, J. 1917b. Radio-active halos. *Nature* 99:456–458, 476–478.

Joly, J. 1923. Radio-active halos. *Proceedings of the Royal Society of London*, Series A102: 682–705.

Joly, J. 1924. The radioactivity of the rocks. *Nature* 114:160–164.

Joplin, G.A. 1931. Petrology of the Hartley district. i. The plutonic and associated rocks. *Proceedings of the Linnean Society of New South Wales* 56:16–59.

Joplin, G.A. 1933. The petrology of the Hartley district. ii. The metamorphosed gabbros and associated hybrid and contaminated rocks. *Proceedings of the Linnean Society of New South Wales* 58:125–158.

Joplin, G.A. 1935. The petrology of the Hartley district. iii. The contact metamorphism of the Upper Devonian (Lambian) series. *Proceedings of the Linnean Society of New South Wales* 60:16–50.

Joplin, G.A. 1936. A comparison of the Rydal and Hartley exogenous contact-zones. *Proceedings of the Linnean Society of New South Wales* 61:151–154.

Joplin, G.A. 1944. Petrology of the Hartley district. v. Evidence of hybridization in the Moyne Farm intrusion: A revision. *Proceedings of the Linnean Society of New South Wales* 69: 129–138.

Joplin, G.A. 1963. *Chemical analyses of Australian rocks. Part I. Igneous and metamorphic rocks. Bulletin 65*. Canberra, Australia: Bureau of Mineral Resources, Geology and Geophysics.

Kerr-Lawson, D.E. 1927. Pleochroic haloes in biotite from near Murray Bay. *University of Toronto Studies in Geology Series* 24:54–71.

Kerr-Lawson, D.E. 1928. Pleochroic haloes in biotite. *University of Toronto Studies in Geology Series* 27:15–27.

Knutson, J., and R.H. Flood. 1988. Ben Bullen plutons, New South Wales: A Carboniferous gabbro-trondhjemite suite. *Australian Journal of Earth Sciences* 35, no.2:245–257.

Laney, R., and A.W. Laughlin. 1981. Natural annealing of pleochroic haloes in biotite samples from deep drill holes, Fenton Hill, New Mexico. *Geophysical Research Letters* 8, no.5:501–504.

Mackay, R.M. 1959. *Geology of the Rydal-Tarana district*. B.Sc. (Hons) Thesis (unpublished), The University of Sydney, Australia.

Mackay, R.M. 1961. The Lambie Group at Mt Lambie. Part I. Stratigraphy and structure. *Proceedings of the Linnean Society of New South Wales* 95: 17–21.

Owen, M.R. 1988. Radiation-damaged halos in quartz. *Geology* 16:529–532.

Packham, G.H., ed. 1968. The geology of New South Wales. *Journal of the Geological Society of Australia* 16, no.1:1–654.

Petford, N., A.R. Cruden, K.J.W. McCaffrey, and J.-L. Vigneresse. 2000. Granite magma formation, transport and emplacement in the earth's crust. *Nature* 408: 669–673.

Pitcher, W.S. 1993. *The nature and origin of granite*. London, United Kingdom: Blackie Academic & Professional.

Raymond, O.L., et al. 1998. Bathurst 1:250 000 Geological Sheet SI/55-08, Map and Explanatory Notes, 2nd edition, Sydney, Australia: Geological Survey of New South Wales, and Canberra: Geoscience Australia.

Scheibner, E., and H. Basden., eds. 1998. Geology of New South Wales – Synthesis. Vol.2 Geological evolution. *Memoir Geology* 13, no.2. Sydney, Australia: Geological Survey of New South Wales.

Scheibner, E., and B.P.J. Stevens. 1974. The Lachlan River Lineament and its relationship to metallic deposits. *Geological Survey of New South Wales, Quarterly Notes* 14: 8–18.

Shaw, S.E., and R.H. Flood. 1993. Carboniferous magmatic activity in the Lachlan and New England Fold Belts. In *New England Orogen, Eastern Australia: Proceedings of the NEO '93 Conference*, ed. P.G. Flood and J.C. Aitchison, pp.113–121. Armidale, NSW, Australia: Department of Geology, University of New England.

Snelling, A.A. 1974. *The geology of the margins of the Bathurst Granite between Sodwalls and Tarana*. B.Sc. (Hons) Thesis (unpublished), The University of New South Wales, Sydney, Australia.

Snelling, A.A. 2000. Radiohalos. In *Radioisotopes and the age of the earth: A young-earth creationist research initiative*, ed. L. Vardiman, A.A. Snelling, and E.F. Chaffin, pp.381–468. El Cajon, California: Institute for Creation Research, and St. Joseph, Missouri: Creation Research Society.

Snelling, A.A. 2005a. Radiohalos in granites: Evidence for accelerated nuclear decay. In *Radioisotopes and the age of the earth: Results of a young-earth creationist research initiative*, ed. L. Vardiman, A.A. Snelling and E.F. Chaffin, pp.101–207. El Cajon, California: Institute for Creation Research, and Chino Valley, Arizona: Creation Research Society.

Snelling, A.A. 2005b. Isochron discordances and the role of inheritance and mixing of radioisotopes in the mantle and crust. In *Radioisotopes and the age of the earth: Results of a young-earth creationist research initiative*, ed. L. Vardiman, A.A. Snelling and E.F. Chaffin, pp.393–524. El Cajon, California: Institute for Creation Research, and Chino Valley, Arizona: Creation Research Society.

Snelling, A.A. 2008a. Catastrophic granite formation: Rapid melting of source rocks, and rapid magma intrusion and cooling. *Answers Research Journal* 1: 11–25. Retrieved from http://www.answersingenesis.org/articles/arj/v1/n1/catastrophic-granite-formation.

Snelling, A.A. 2008b. Testing the hydrothermal fluid transport model for polonium radiohalo formation: The Thunderhead Sandstone, Great Smoky Mountains, Tennessee—North Carolina. *Answers Research Journal* 1:53–64. Retrieved from http://www.answersingenesis.org/articles/arj/v1/n1/testing-radiohalos-model.

Snelling, A.A. 2008c. Radiohalos in the Cooma Metamorphic Complex, New South Wales, Australia: The mode and rate

of regional metamorphism. In *Proceedings of the Sixth International Conference on Creationism*, ed. A.A. Snelling, pp. 371–387. Pittsburgh, Pennsylvania: Creation Science Fellowship; Dallas, Texas: Institute for Creation Research.

Snelling, A.A. 2008d. Radiohalos in the Shap Granite, Lake District, England: Evidence that removes objections to Flood geology. In *Proceedings of the Sixth International Conference on Creationism*, ed. A.A. Snelling, pp. 389–405. Pittsburgh, Pennsylvania; Creation Science Fellowship, and Dallas, Texas: Institute for Creation Research.

Snelling, A.A., and M.H. Armitage. 2003. Radiohalos: A tale of three granitic plutons. In *Proceedings of the Fifth International Conference on Creationism*, ed. R.L. Ivey, pp. 243–267. Pittsburgh, Pennsylvania: Creation Science Fellowship.

Snelling, A.A., J.R. Baumgardner, and L. Vardiman. 2003. Abundant Po radiohalos in Phanerozoic granites and timescale implications for their formation. *EOS, Transactions of the American Geophysical Union 84*:46. Fall Meeting Supplement, Abstract V32C-1046.

Snelling, A.A., and D. Gates. 2009. Implications of polonium radiohalos in nested plutons of the Tuolumne Intrusive Suite, Yosemite, California. *Answers Research Journal* 2: 53–77. Retrieved from http://www.answersingenesis.org/articles/arj/v2/n1/radiohalos-in-yosemite-granites.

Snelling, A.A., and J. Woodmorappe. 1998. The cooling of thick igneous bodies on a young earth. In *Proceedings of the Fourth International Conference on Creationism*, ed. R.E. Walsh, pp. 527–545. Pittsburgh, Pennsylvania: Creation Science Fellowship.

Stark, M. 1936. Pleochroitische (radioaktive) höfe ihre verbreitung in den gesteinen und veränderlickheit. *Chemie der Erde* 10:566–630.

Turner, F.J. 1968. *Metamorphic petrology: Mineralogical and field aspects*. New York, New York: McGraw-Hill.

Tuttle, O.F. 1955. The origin of granite. *Scientific American* 192. no. 4:77–82.

Tuttle, O.F., and N.L. Bowen 1958. Origin of granite in the light of experimental studies in the system $NaAlSi_3O_8$-$KAlSi_3O_8$-SiO_2-H_2O. *GSA Memoirs* 74:1–146. Boulder, Colorado: Geological Society of America.

Vallance, T.G. 1969. Plutonic and metamorphic rocks. In *The geology of New South Wales*, ed. G.H. Packham. *Journal of the Geological Society of Australia* 16, no. 1:180–200.

Vardiman, L.., A.A. Snelling, and E.F. Chaffin, eds. 2005. *Radioisotopes and the age of the earth: Results of a young earth creationist research initiative*. El Cajon, California: Institute for Creation Research and Chino Valley, Arizona: Creation Research Society.

Washington, H.S. 1917. *Chemical analyses of igneous rocks*. Professional Paper 99. Washington DC: U.S. Geological Survey.

Wiman, E. 1930. Studies of some Archaean rocks in the neighbourhood of Uppsala, Sweden, and their geological position. *Bulletin of the Geological Institute, University of Uppsala* 23:1–170.

Wise, K.P. 1989. Radioactive halos: Geological concerns. *Creation Research Society Quarterly* 25:171–176.

Young, D.A., and R.F. Stearley. 2008. *The Bible, rocks and time: Geological evidence for the age of the earth*. Downers Grove, Illinois: InterVarsity Press.